

# Towards Label-efficient Automatic Diagnosis and Analysis: A Comprehensive Survey of Advanced Deep Learning-based Weakly-supervised, Semi-supervised and Self-supervised Techniques in Histopathological Image Analysis

Linhao Qu, Siyu Liu, Xiaoyu Liu, Manning Wang<sup>†</sup>, Zhijian Song<sup>‡</sup>

Shanghai Key Lab of Medical Image Computing and Computer Assisted Intervention, Digital Medical Research Center, School of Basic Medical Science, Fudan University, Shanghai 200032, China

E-mail: {1hqu20, mnwang, zjsong}@fudan.edu.cn.

**Abstract.** Histopathological images contain abundant phenotypic information and pathological patterns, which are the gold standards for disease diagnosis and essential for the prediction of patient prognosis and treatment outcome. In recent years, computer-automated analysis techniques for histopathological images have been urgently required in clinical practice, and deep learning methods represented by convolutional neural networks have gradually become the mainstream in the field of digital pathology. However, obtaining large numbers of fine-grained annotated data in this field is a very expensive and difficult task, which hinders the further development of traditional supervised algorithms based on large numbers of annotated data. More recent studies have started to liberate from the traditional supervised paradigm, and the most representative ones are the studies on weakly supervised learning paradigm based on weak annotation, semi-supervised learning paradigm based on limited annotation, and self-supervised learning paradigm based on pathological image representation learning. These new methods have led a new wave of automatic pathological image diagnosis and analysis targeted at annotation efficiency. With a survey of over 130 papers, we present a comprehensive and systematic review of the latest studies on weakly supervised learning, semi-supervised learning, and self-supervised learning in the field of computational pathology from both technical and methodological perspectives. Finally, we present the key challenges and future trends for these techniques.

*Keywords:* histopathological images, automatic analysis, deep learning

<sup>‡</sup> Corresponding Author.

## 1. Introduction

Histopathological images contain abundant phenotypic information and pathological patterns, which are the gold standards for disease diagnosis and essential for the prediction of patient prognosis and treatment outcome (Myronenko *et al.* 2021, Wang *et al.* 2019, Srinidhi *et al.* 2021). For clinical diagnosis, experienced pathologists usually require exhaustive examination and interpretation of hematoxylin-eosin-stained (H&E) tissue slides under a high magnification microscope, including differentiation of tumor areas from large areas of normal tissues, elaborate grading of tumors, and detailed assessment of tumor progression and invasion (e.g., presence of invasive carcinoma or proliferative changes, etc.). This is a highly time-consuming and labor-intensive task, and for example, it usually takes an experienced histopathologist 15 to 30 minutes to examine a complete slide (Wang *et al.* 2019). Moreover, even an experienced pathologist may not be able to accurately determine the deep features hidden in the pathological images, such as predicting lymph node metastasis and prognosis from the primary lesion. Therefore, computer-assisted automatic analysis techniques for histopathological images are in urgent need in clinical practice.

With the advent and development of digital slide scanners in the past two decades, tissues on biopsies can be converted into digital whole slide images (WSIs) that fully preserve the original tissue structure, laying the foundation for automatic pathological image analysis. Early studies in the field of digital pathology diagnosis primarily focused on extracting hand-crafted features from manually selected regions of interest (ROI) by pathologists (Jafari *et al.* 2003, Basavanhally *et al.* 2013, Mercan *et al.* 2017, Yu *et al.* 2016, Luo *et al.* 2017, Qaiser *et al.* 2016) and using machine learning methods (Doyle *et al.* 2007, Rajpoot *et al.* 2004, Qureshi *et al.* 2008, Doyle *et al.* 2006) for automatic analysis and diagnosis. In this regard, Gurcan *et al.* 2009 and Madabhushi *et al.* 2016 have presented an elaborate review.

In recent years, thanks to the powerful and automatic feature extraction and inductive bias capability, deep learning methods represented by Convolutional Neural Network (CNN) have gradually become the mainstream in the field of digital pathology. However, a major challenge is the huge size of WSIs, typically reaching  $100000 \times 100000$  pixels at the highest resolution, which prevents the direct use of the entire WSIs as the input to deep learning models. Therefore, when using CNNs to process pathological images, WSIs are usually tiled into many small patches to reduce the computational burden. Earlier studies usually adopted a strongly supervised approach based on these patches to train the network and perform the corresponding classification (Cruz-Roa *et al.* 2014, Cruz-Roa *et al.* 2017, Wei *et al.* 2019, Ehteshami *et al.* 2018, Nagpal *et al.* 2019, Shaban *et al.* 2019, Halicek *et al.* 2019) and segmentation tasks (Chen *et al.* 2017, Gu *et al.* 2018, Swiderska *et al.* 2019). In these works, detailed patch-level annotation is essential, e.g., supervised classification problems require pathologists to give detailed class labels for each patch, and segmentation problems require pathologists to give more detailed pixel-level annotation for each patch.

Although supervised deep learning methods have achieved unprecedented success in digital pathology, they share a common drawback: they all require large amounts of high-quality fine-grained labeled data (patch-level labeled data for classification problems or pixel-level labeled data for segmentation problems) for training. Unfortunately, in the field of digital pathology, obtaining a large amount of data with fine-grained annotation is a very expensive and challenging task, mainly because 1) only experienced pathologists can perform the annotation, and these pathologists are scarce; 2) histopathological images often contain complex and diverse instances of objects, resulting in a large amount of time-consuming and laborious manual annotation effort (Tajbakhsh *et al.* 2020, Yang *et al.* 2017, Srinidhi *et al.* 2021). Arguably, the lack of a large amount of annotated data limits the application of deep learning techniques in computational pathology. For this reason, some new studies have recently attempted to liberate from the traditional strongly supervised paradigms, the most representative of which are the weakly supervised learning paradigm based on weak annotations, the semi-supervised learning paradigm based on limited annotations, and the self-supervised paradigm based on the representation learning of pathological images.

The weakly supervised learning paradigm no longer requires pathologists to give annotations of all pixels or regions on the entire WSI, but only class labels or sparse region annotations on the entire WSI; the semi-supervised learning paradigm no longer requires pathologists to give fine-grained annotations of a large amount of data, but only a small fraction of fine-grained labeled data and a large amount of unlabeled data; while the self-supervised learning paradigm can create supervised information through a large amount of unlabeled data for self-supervised training to learn an accurate feature representation of the data. In the process of training with limited labeled data, using the features trained by self-supervised learning to determine the initial model weights can significantly improve the performance of the model. Therefore, weakly supervised learning, semi-supervised learning and self-supervised learning are leading a new study direction of the automatic diagnosis and analysis for pathological images.

However, there are very few related reviews. Srinidhi *et al.* 2021 reviewed representative supervised learning, weakly supervised learning, unsupervised learning, and transfer learning studies in the field of computational pathology until December 2019. Rony *et al.* 2019 reviewed representative weakly supervised learning studies until 2020. Nevertheless, in recent years, deep learning techniques have been developing rapidly and the new techniques continue to emerge. Therefore, a review regarding the applications of these techniques in the automatic diagnosis of pathological images has important theoretical value and clinical significance.

In this review, we summarize more than 130 recent technical studies systematically on weakly supervised learning, semi-supervised learning, and self-supervised learning in the field of computational pathology. We performed this extensive review by searching Google Scholar, PubMed, and arXiv for papers including keywords such as ("deep learning" or "weakly supervised learning" or "semi-supervised learning" or "self-supervised learning") and ("digital pathology" or "histopathology" or "computational

pathology”). Notably, on the one hand, we focus on papers presenting novel techniques and theories with high impact (h-index, citations and impact factors of journals), thus we concentrate more on studies published in top conferences (including CVPR, NeurIPS, MICCAI, ISBI, MIDL, IPMI, AAAI, ICCV, ECCV, etc.) and top journals (including TPAMI, TMI, MIA, etc.) on weakly supervised, semi-supervised, and self-supervised learning in the field of computational pathology. On the other hand, since technical research in this area is growing rapidly and more new techniques have been proposed, we mainly cover papers published in 2019-2021. On the other hand, we also present a meticulous summary of the disease types, tasks, datasets, and performance covered by these papers. In total, this review contains more than 200 relevant articles. This review adheres to PRISMA (Rethlefsen *et al.* 2021) guideline.

The rest of the paper is organized as follows: Section 2 expounds a general overview of the weakly supervised, semi-supervised, and self-supervised learning paradigms in the context of computational pathology; Section 3 includes a detailed review of the weakly supervised (Section 3.1), semi-supervised (Section 3.2), and self-supervised (Section 3.3) learning paradigms; we discuss the three learning paradigms and their future trends in Section 4, and conclude the whole paper in Section 5. The list of all the acronyms used in this review is shown in Table 1.

Table 1: List of all the acronyms in this review.

Full Name	Acronyms	Full Name	Acronyms
Area Under ROC Curve	AUC	Graph Neural Network	GNN
Auxiliary Classifier Generative Adversarial Networks	AC-GAN	Hematoxylin-Eosin-Stained	H&E
Average Hausdorff Distance	AHD	Magnification Prior Contrastive Similarity	MPCS
Average Jaccard Index	AJI	Mean Average Precision	MAP
Calinski-Harabaz Index	CHI	Mean Teachers	MT
Contrastive Predictive Coding	CPC	Microsatellite Instability	MSI
Convolutional Autoencoder	CAE	Multiple Instance Fully Convolutional Network	MI-FCN
Convolutional Neural Network	CNN	Multiple Instance Learning	MIL
Deep Learning Hashing	DLH	Noise Contrastive Estimation	NCE
Deformation Representation Learning	DRL	Percentage Of Tumor Cellularity	TC
Diffusion-Convolutional Neural Networks	DCNNs	Recurrent Neural Network	RNN
Dual-Stream Multiple Instance Learning	DSMIL	Regions Of Interest	ROI
Expectation-Maximization	EM	Resolution Sequence Prediction	RSP
Exponential Moving Average	EMA	Silhouette Index	SI
Focal-Aware Module	FAM	Support Vector Machines	SVM
Frechet Inception Distance	FID	Temporal Ensembling	TE
Generative Adversarial Networks	GAN	The Cancer Genome Atlas Program	TCGA
Graph Convolutional Neural Network	GCN	Whole Slide Images	WSI

## 2. Overview of Learning Paradigms and Problem Formulation

In this section, we provide a general overview and problem formulation of the three learning paradigms reviewed in this paper, and compare them with the traditional strongly supervised paradigm. To make the description more specific and vivid, we present an example of accurately classifying normal and cancerous tissues in a WSI, as shown in Figure 1. The raw data for this example WSI comes from a study on predicting lymph node metastasis in breast cancer using deep learning (Bejnordi *et al.* 2017a). We also intuitively compare and summarize these paradigms in Table 2.

Given a dataset  $W = \{W_i\}_{i=1}^N$  consisting of  $N$  WSIs, each WSI  $W_i$  is now cut into patches  $\{p_{i,j}, j = 1, 2, \dots, n_i\}$ , and  $n_i$  is the number of patches cut out of  $W_i$ . In

the supervised learning paradigm, a large number of patches with fine-grained labels are available for training, so each patch is given a label  $y_{i,j} = \mathbb{R}^C$ , and  $C$  denotes the possible class. For example, in the binary classification task,  $C$  takes the scalar form  $\{0, 1\}$  while in the regression task,  $C$  takes the form of a continuous set of real numbers  $\mathbb{R}$ . The goal of the supervised learning paradigm is to train a model  $f_\theta : x \rightarrow y$  to optimally predict the labels  $y_{i,j}$  of the unknown patches  $p_{i,j}$  in the test WSI based on the loss function  $\mathcal{L}$ . Figure 1 (a) illustrates the main process of this paradigm. During training, the model is trained in a supervised manner using patches cut out of the training WSIs and their labels (green for negative and red for positive) by pathologists; during testing, the trained model is used to predict the labels of the patches cut out of the unseen test WSIs.

In the weakly supervised learning paradigm, the label  $y_{i,j}$  of each patch is typically unknown, while only the label of each WSI is available, and thus the traditional strongly supervised learning paradigm cannot work. In this review, we focus on the most dominant weakly supervised paradigm currently used in computational pathology, the deep multiple instance learning (MIL) approach. In MIL, each WSI is considered as a bag containing many patches (also called instances). If a WSI (bag) is labeled as disease-positive, then at least one patch (instance) in that WSI is disease-positive; if a WSI is disease-negative, then all patches in that WSI are negative. The relationship between a WSI (bag) and its patches (instances) can be expressed mathematically as follows.

Given a dataset  $W = \{W_i\}_{i=1}^N$  consisting of  $N$  WSIs, each image  $W_i$  has a corresponding label  $Y_i \in \{0, 1\}$ ,  $i = \{1, 2, \dots, N\}$ . Now each WSI  $W_i$  is cut into small patches  $\{p_{i,j}, j = 1, 2, \dots, n_i\}$  without overlapping each other, and  $n_i$  is the number of patches. Where, all patches  $\{p_{i,j}, j = 1, 2, \dots, n_i\}$  in  $W_i$  form a bag, the bag-level label is the label  $Y_i$  of  $W_i$ , and each small patch is called an instance of this bag, while the instance-level label  $y_{i,j}$  and its corresponding bag-level label  $Y_i$  has the following relationship:

$$Y_i = \begin{cases} 0, & \text{if } \sum_j y_{i,j} = 0 \\ 1, & \text{else} \end{cases} \quad (1)$$

It means that the labels of all instances in the negative bag are negative, while at least one positive instance exists in the positive bag and the labels of instances  $y_{i,j}$  are unknown.

As shown in Figure 1 (b), generally, there are two main goals of deep learning-based WSI analysis, one is global slide classification, i.e., to accurately classify each WSI, and the other is positive patch localization, i.e., to accurately classify each instance in positive bags. A review of the current state-of-the-art weakly supervised learning methods is presented in Section 3.1.

In the semi-supervised learning paradigm, we only have a very small number of patches with labels, in addition to a large number of unlabeled patches that can also be used for training. Therefore, the main goal of the semi-supervised learning paradigm

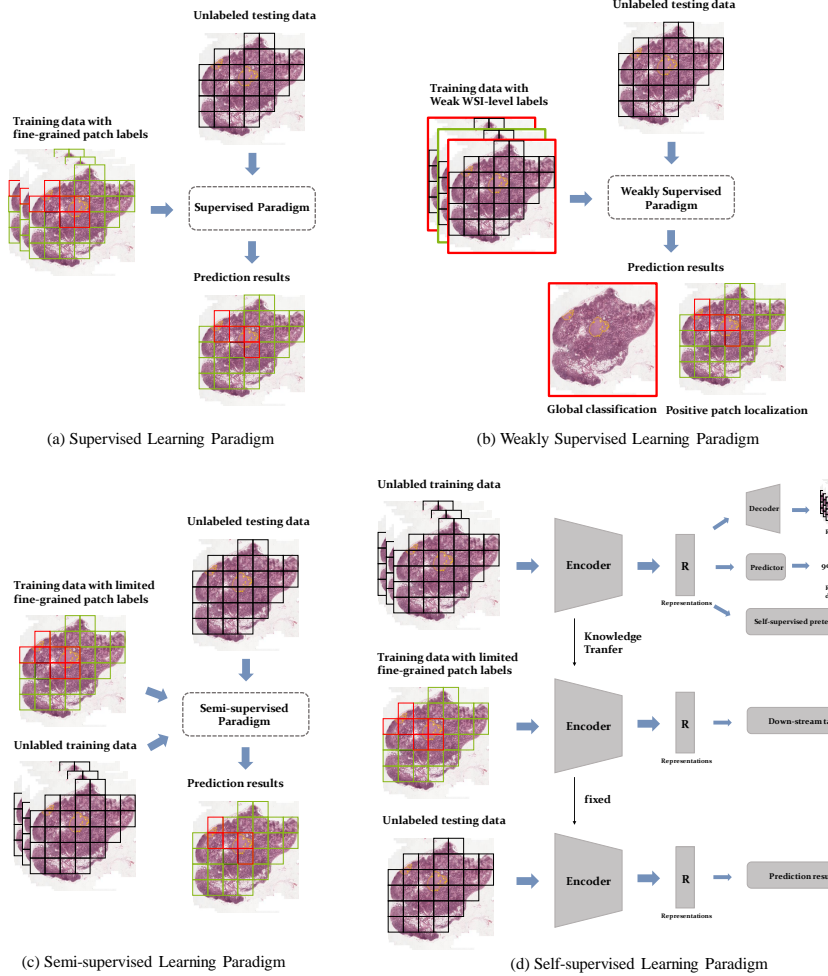


Figure 1: General overview of the learning paradigms reviewed in this paper, depicted as an example of classifying normal tissue (green) and cancerous tissue (red) in a WSI. Note that the training data and testing data in this figure are used for description only and are not necessarily the real case. (a) Supervised learning paradigm. (b) Weakly Supervised learning paradigm. (c) Semi-supervised learning paradigm. (d) Self-supervised learning paradigm.

is how to use the unlabeled data to improve the performance of the models trained with limited labeled data. As shown in Figure 1 (c), in contrast to the supervised learning paradigm, the semi-supervised learning paradigm makes use of a large amount of unlabeled data while training with the labeled data. During testing, the trained model is used to predict the labels of the patches in test WSIs. See Section 3.2 for a detailed review of the semi-supervised learning methods.

Self-supervised learning is a hybrid learning approach, which combines unsupervised and supervised learning paradigms in a pre-training and fine-tuning manner. The aim is to get better results of supervised training through generating supervised information from a large amount of unlabeled data, which can learn better feature

Table 2: Intuitive summary and comparison of the four paradigms.

Methods	Input	Suitable tasks	Technical paradigms	Strengths	Weaknesses
Supervised learning paradigm	A large number of small patches (tiled from WSIs) with fine-grained labels	WSI-level and patch-level classification/segmentation/regression	-	Broad application, effective and simple training	Require large amount of fine-grained labeled data
Weakly Supervised learning paradigm	Entire WSIs with overall labels or sparse labels	WSI-level classification/segmentation/regression, Patch-level coarse-grained localization	Instance-based approach, Bag-based approach, Hybrid approach	No need for fine-grained annotation, effectively reduce the burden of data annotation	Achieve limited performance for fine-grained tasks
Semi-supervised learning paradigm	A limited number of small patches (tiled from WSIs) with fine-grained labels	WSI-level and patch-level classification/segmentation/regression	Pseudo-labelling-based approach, Consistency-based approach, Graph-based approach, Unsupervised-preprocessing-based approach, GAN-based approach and others	Require only a small amount of fine-grained annotation, effectively reduce the burden of data annotation	Need to satisfy various semi-supervised assumptions
Self-supervised learning paradigm	A large number of small patches (tiled from WSIs) without labels	Patch-level feature representations, Multiple related down-stream tasks	Predictive approach, Generative approach, Contrastive approach, Hybrid approach	Efficiently extract image features from a large amount of unsupervised data, effectively reduce the data annotation burden	May result in information loss when the extracted features are not applicable to downstream tasks

representations, and can avoid manual annotation in the subsequent tasks. Due to the small amount of annotated data, it is not sufficient to use these data directly to train the model. Therefore, the self-supervised learning paradigm first learns a primary feature representation from a large amount of unlabeled data, which is called the pre-training process. The feature representations learned in the self-supervised auxiliary tasks are then transferred as initial weights for retraining in downstream tasks using limited labeled data, which is called the fine-tuning process. In this way, the primary feature representations can effectively help the network to achieve an effective training result with less labeled data.

As shown in Figure 1 (d), the pre-training process of the self-supervised learning paradigm is typically performed through self-supervised auxiliary tasks. In the self-supervised auxiliary tasks, certain inherent properties of the unlabeled data are first utilized to generate supervised information, and then the network is trained by the self-supervised information, such as self-reconstruction, random rotation followed by angle prediction, color information discarding followed by colorization, and patch position disruption followed by restoration. Once accomplishing these self-supervised auxiliary tasks, the effective feature representations can be extracted. The fine-tuning process of self-supervised learning is done in the downstream tasks. During the fine-tuning process, a small amount of labeled data is used to perform the supervised training, and the model is not trained from scratch, but is re-trained using the feature representations learned in the auxiliary tasks as the initial weights of the network. Finally, the trained network is used for testing. A review of the state-of-the-art self-supervised learning methods is presented in Section 3.3.

### 3. Paradigms

#### 3.1. Weakly Supervised Learning Paradigm

In this section, we provide a comprehensive review of the primary deep multiple instance learning (MIL) methods currently used in the weakly supervised learning paradigm for computational pathology. In MIL, each WSI is considered as a bag containing many patches (also called instances). If a WSI (bag) is labeled disease-positive, then at least one patch (instance) in that WSI is disease-positive; if a WSI is disease-negative, then all patches in that WSI are negative. There are two main goals in deep learning-based WSI analysis: the global slide classification, which can accurately predict the labels of each WSI, and positive patch localization, which can accurately predict the labels of each patch in positive bags.

We categorize the current deep MIL methods for WSI analysis into instance-based methods, bag-based methods, and hybrid methods. Our categorization is mainly based on whether the methods contain an instance classifier or a bag classifier, i.e., instance-based methods contain only an instance classifier; bag-based methods contain only a bag classifier; while hybrid methods contain both an instance classifier and a bag classifier. In this way, the categories clearly cover almost all current deep MIL methods for WSI analysis. A diagram of the three methods above is shown in Figure 2. The detailed literatures in this section are summarized in Table 3.

##### 3.1.1. Instance-based Approach

The main idea of the instance-based approach is to train a good instance classifier to accurately predict the potential labels of instances in each bag, and then use MIL-pooling to aggregate the predictions of all instances in each bag to obtain the prediction of the bag. The details are shown in Figure 2 (a). Since the true labels of each instance are unknown, these approaches usually first assign the labels of each instance with their corresponding bags as the pseudo labels (i.e., all instances in a positive bag are given positive labels, and all instances in a negative bag are given negative labels), and then train the instance classifier using a supervised way until it converges. The loss function is usually the cross-entropy function defined between the predictions of the instance classifier and the pseudo labels. After training, the instance classifier is used to make predictions for all instances in the test bag, and then the predictions of each instance are aggregated to obtain the prediction of the bag, and this aggregation process is called MIL-pooling. Commonly used MIL pooling methods include Mean-pooling (Wang *et al.* 2018), Max-pooling (Feng *et al.* 2017, Wang *et al.* 2018, Wu *et al.* 2015), Voting (Cruz-Roa *et al.* 2014), log-sum-exp-pooling (Ramon *et al.* 2000), Noisy-or-pooling (Maron *et al.* 1997), Noisy-and-pooling (Kraus *et al.* 2016), and Dynamic pooling (Yan *et al.* 2018) among others.

Instance-based approach is more common in early studies, and its main advantage lies in the direct prediction of each instance so that the localization task can be performed conveniently. However, it has two major drawbacks. First, since the true

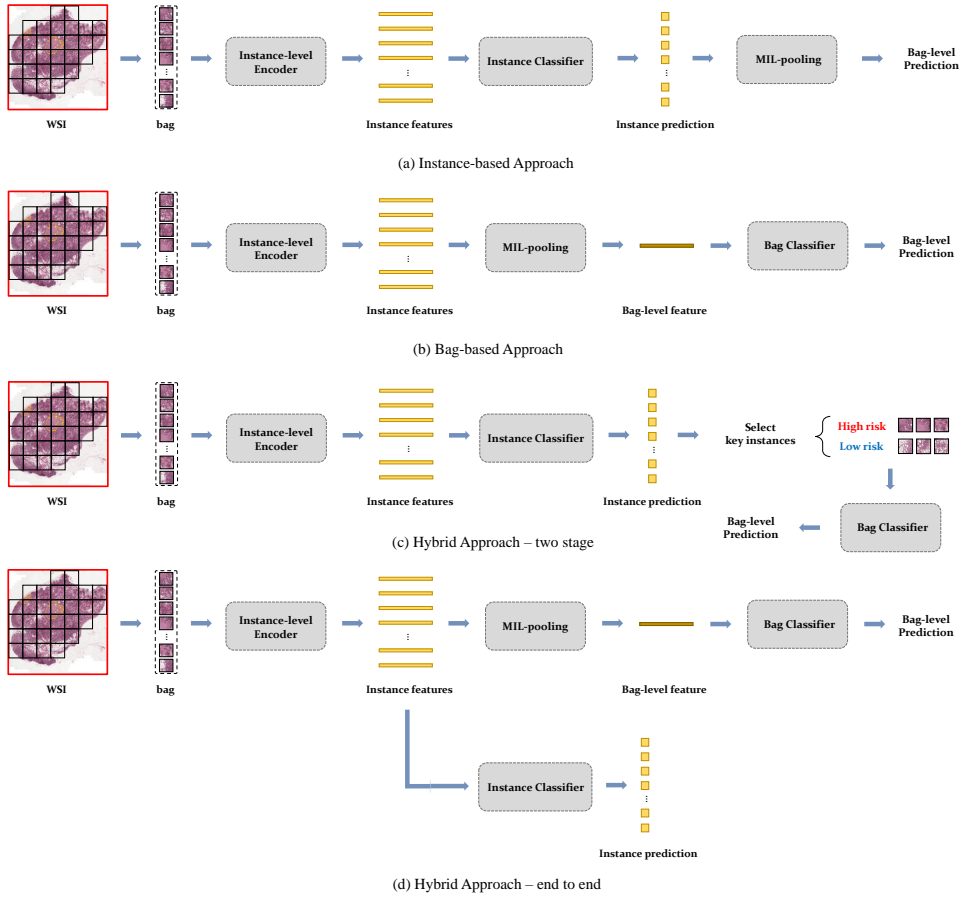


Figure 2: Overview of multiple instance learning methods. (a) Instance-based Approach. (b) Bag-based Approach. (c) Two-stage Hybrid Approach. (d) End-to-End Hybrid Approach.

labels of each instance in the positive bags are not necessarily all positive, the pseudo labels assigned to the instances in the positive bags are noisy, which will lead to inaccurate training of the instance classifier; Second, the MIL-pooling method, which aggregates the predictions of instances in each bag, is manually designed and non-trainable, making it less flexible and robust. Therefore, the performance of these methods is usually limited.

### 3.1.2. Bag-based Approach

The main idea of the bag-based approaches is to first extract the features of each instance in a bag using shared instance-level feature extractors, then use MIL-pooling to aggregate the instance-level features to obtain the bag-level features, and then train the bag classifier in a supervised manner until it converges. The specific diagram is shown in Figure 2 (b). The loss function is usually defined as the cross-entropy loss between the predictions of the bag classifier and the true bag labels.

MIL-pooling also exists in bag-based methods, but unlike instance-based methods,

MIL-pooling here aggregates not the predictions of instances, but the features of instances. Mean-pooling, Max-pooling and other aggregation methods can also be used as aggregation methods for instance features, but their drawbacks remain, i.e., they cannot be trained and adjusted adaptively, so they are often not flexible enough.

The key of the bag-based methods is the training of the bag classifier. Since the true labels of the bags are available, there is no noise in their training process, so these methods tend to be more accurate than instance-based methods in bag classification. However, a serious problem of the bag-based approaches is that they cannot perform the localization task easily. Furthermore, the aggregation functions for instance features are not flexible enough to show the contribution of different instances to bag classification.

*Attention-based Approach* Ilse *et al.* 2018 have alleviated these dilemmas. They first proposed to use the trainable attention mechanism to aggregate instance features, and started a wave of study on attention-based aggregation methods by subsequent bag-based methods. They trained both the instance-level feature extractor and a bag-level classifier using an end-to-end manner, and used the attention mechanism to aggregate the features and measure the significance of each instance. Tu *et al.* 2019 proposed a new end-to-end graph neural network (GNN) for instance aggregation. This work is the first GNN-based MIL work. Hashimoto *et al.* 2020 proposed a novel end-to-end method for cancer subtype classification by combining MIL, domain adversarial and multiscale learning frameworks. Yao, Zhu *et al.* 2017, 2020 proposed a deep attention guided MIL framework for cancer survival analysis. They first used a pre-trained model from ImageNet (Deng *et al.* 2009) to extract the features of instances in each bag, and then used K-means algorithm to cluster the instances in each bag to obtain the phenotypic patterns, and then applied attention mechanism to aggregate the features of these patterns and performed prediction.

*Self-supervised pre-training-based Approach* Due to the extremely large size of WSIs and the large number of instances cut out, direct end-to-end training of all instances is easily limited by computational resources. Therefore, some studies first use advanced self-supervised pre-training methods to characterize each instance and then perform subsequent training. Lu *et al.* 2019 first proposed to obtain instance-level feature representations by self-supervised contrastive predictive coding (CPC), and then used the attention-based MIL method for instance aggregation to perform bag-level classification. This is the first MIL study using self-supervised contrastive learning. Zhao *et al.* 2020 used a pre-trained VAE-GAN (Larsen *et al.* 2016) to extract instance-level features, and then used GNN to aggregate instance features and perform bag-level classification. Li *et al.* 2021 proposed DSMIL, where they used contrastive pre-training (Chen *et al.* 2020) to obtain the instance features, and then proposed the masked non-local operation-based dual-stream aggregator to perform both instance-level classification and bag-level classification.

*Transformer based Approach* In MIL-based WSI analysis, not only the contribution of different instances to bag classification should be considered, the relationships among different instances should also be fully explored, because different instances in a WSI are not isolated from each other, but have strong correlation. To address this issue, Shao *et al.* 2021 and Li *et al.* 2021 et al. used Transformer-based architectures to aggregate instances and both achieved promising results. The former designed a Transformer-based correlated MIL framework to explore the morphological and spatial information among different instances and provided related proofs. The latter presented a MIL framework based on the deformable transformer and convolutional layers.

### 3.1.3. Hybrid Approach

The hybrid approach combines the advantages of the above two approaches. It trains both the instance-level classifier and the bag-level classifier, and uses the former to predict the instance-level results while the latter for bag-level results. Overall, there are two types of the hybrid approaches. One is the two-stage approach and the other is the end-to-end approach.

*Two-stage Hybrid Approach* The two-stage hybrid approach generally trains the instance classifier by assigning each instance in each bag with their corresponding bag labels as pseudo labels, and then trains the bag classifier to complete the bag classification based on the predictions of the instance classifier. Some studies have also attempted to select the key instances in each bag based on the predictions of the instance classifier, and then train the bag classifier based on these key instances. The specific diagram is shown in Figure 2 (c). Hou *et al.* 2016 proposed a new Expectation-Maximization (EM) based model. They selected discriminative instances based on spatial relationship to train the instance classifier and fed the histogram of instance predictions into the multiclass logistic regression model and the SVM model (Chang *et al.* 2011) for bag prediction. Campanella *et al.* 2019 first selected key instances with the maximum prediction probability of the instance classifier in the current iteration and assigned pseudo labels of the corresponding bag labels to them. Then they fed the features of these key instances into the recurrent neural network (RNN) to perform the aggregation and prediction of the bags. Wang *et al.* 2019 selected key instances based on the predictions of positive instance probability and fed their features into the global feature descriptor and used the random forest algorithm to classify the bags. Chen *et al.* 2021 proposed a focal-aware module (FAM) and used thumbnails of WSI to automatically estimate the key regions associated with the diagnosis. Then, the instance features at different scales were extracted based on these key regions and aggregated using GNN to perform the bag classification.

*End-to-end Hybrid Approach* The end-to-end hybrid approach generally trains the instance-level classifier and the bag-level classifier at the same time. A common approach is to train the two classifiers simultaneously by assigning each instance the

corresponding bag labels as pseudo labels on top of the bag classifier. Some studies also train the instance classifier to select the key instances in an epoch first, and then train the bag classifier after aggregating the instance features. The specific diagram is shown in Figure 2 (d). Shi *et al.* 2020 proposed loss-based attention MIL. They added an instance-level loss function weighted by the instance attention scores based on AB-MIL (Ilse *et al.* 2018) as a regularization term to improve the recall of instances and used consistency constraints to smooth the training process to improve the generalization ability. Chikontwe *et al.* 2020 combined top-k instance selection, instance-level representation learning, and bag-level representation in an end-to-end framework. Sharma *et al.* 2021 also combined instance selection, instance-level representation learning and bag-level representation in an end-to-end framework. Unlike (Chikontwe *et al.* 2020), they proposed to use a clustering-based sampling method to select key instances. Lu *et al.* 2021 also proposed a MIL framework based on clustering and attention mechanisms. They selected the instances with the largest and smallest attention scores in the current bag for clustering to enhance the learning of feature space. Myronenko *et al.* 2021 proposed a MIL framework combining the Transformer and CNN architectures to compute the interrelationships between instances and aggregate the instances features to accomplish the bag classification. They added the instance loss to assist the optimization process.

### 3.1.4. Representative Clinical Studies

A large number of outstanding studies have been dedicated to address significant clinical problems using weakly supervised methods. For example, Coudray *et al.* 2018 et al. developed deep learning models for accurate prediction of cancer subtypes and genetic mutations and sparked the whole field of weakly supervised computational pathology. Naik *et al.* 2020 et al. presented an attention-based deep MIL framework to predict directly estrogen receptor status from H&E slices. Another typical clinical work comes from Tomita *et al.* 2019, who proposed a grid-based attention network to perform 4-class classification of high-resolution endoscopic esophagus and gastroesophageal junction mucosal biopsy images from 379 patients. Skrede *et al.* 2020 developed a multi-scale deep MIL-based model to analyze conventional HE-stained slides and developed a model that can effectively predict the prognosis of patients after colorectal cancer surgery. Another gastrointestinal tract oncology study (Kather *et al.* 2019) predicted microsatellite instability (MSI) based on a deep MIL model directly on HE-stained slides. Currently, weakly supervised deep-learning models for digital pathological analysis has been applied in a wide range of cancer types including breast, colorectal, lung, liver, cervical, thyroid, and bladder cancers (Coudray *et al.* 2018, Chaudhary *et al.* 2018, Wessels *et al.* 2021, Campanella *et al.* 2019, Anand *et al.* 2021, Yang *et al.* 2022, Li *et al.* 2021, Saillard *et al.* 2020, Velmahos *et al.* 2021, Woerl *et al.* 2020).

Table 3: List of literatures in the weakly supervised learning section.

Reference	Approach	Disease Type	Staining	Task	Dataset	Dataset Scale	Dataset Link	Performance
Yan et al. (2018)	Instance-based	Breast Cancer Diabetes (from eye fundus images)	H&E	Benign and malignant classification	UCSB breast dataset; Messidor dataset	358 cases 1200 cases	Kandemir et al. (2014) Desenvee et al. (2014)	Accuracy: 0.927 Accuracy: 0.740
Kraus et al. (2016)	Instance-based	Breast Cancer	H&E	Classification of 12 distinct categories	Broad Biostorage Biobank Collection (BBBG021v1) dataset	340 cases	Ljosa et al. (2012)	Accuracy: 0.056 for full image; 0.971 for treatment influence
Cruz-Roa et al. (2014)	Instance-based	Breast Cancer	H&E	Automatic detection of invasive ductal carcinoma	Clinical histopathology dataset collected from multiple hospitals	162 cases	Galwey et al. (2009)	Accuracy: 0.842
Ilie et al. (2018)	Bag-based	Breast Cancer Colon Cancer Diabetes (from eye fundus images)	H&E	Automatic detection of cancer regions from fundus images	Breast cancer dataset; Colon cancer dataset	158 cases 100 cases	Srinivasanwala et al. (2016)	Accuracy: 0.755
Tu et al. (2019)	Bag-based	Breast Cancer	H&E	Detecting diabetic fundus images with labeled retinal fundus images	CancerGenome Atlas (TCGA) dataset	1200 cases	Desenvee et al. (2014)	Accuracy: 0.904
Hasimotto et al. (2020)	Bag-based	Malignant Lymphoma	H&E	Classification of malignant lymphoma subtypes	Clinical histopathology dataset collected from multiple hospitals	196 cases	Galwey et al. (2009)	Accuracy: 0.742
Yao et al. (2020)	Bag-based	Lung Cancer	H&E	Cancer survival prediction	National Lung Screening Trial (NLST) dataset; Molecular and Cellular Oncology (MCO) dataset	387 cases	Team et al. (2011)	Accuracy: 0.871
Li et al. (2019)	Bag-based	Colorectal Cancer	H&E	Classification of normal or benign	Ward and Hawkins (2015)	1,446 cases	AUC: 0.713	Accuracy: 0.927
Zhao et al. (2020)	Bag-based	Breast Cancer Colon Adenocarcinoma	H&E	Prediction of lymph node metastasis	Aresta et al. (2019)	400 cases	AUC: 0.95	
Li, Li and Elicitri (2021)	Bag-based	Breast Cancer	H&E	Detection of lymph node metastases	Kandemir et al. (2014)	45 cases	AUC: 0.6761	
Shao et al. (2021)	Bag-based	Lung Cancer	H&E	Diagnosis of lung cancer subtypes	Bejnordi et al. (2017b)	400 cases	AUC: 0.892	
Li, Yang, Zhao and Yao (2021)	Bag-based	Breast Cancer Lung Cancer Kidney Cancer Prost. Cancer Glioma	H&E	Detection of lymph node metastases	https://portal.gdc.cancer.gov/	1054 cases	AUC: 0.971	
Hen et al. (2016)	Hybrid	Lung Cancer Prostate Cancer Skin Cancer	H&E	Diagnosis of lung cancer subtypes	Bejnordi et al. (2017b)	400 cases	AUC: 0.8857	
Companella et al. (2019)	Hybrid	Breast Cancer Lung Cancer Breast Cancer Glioma	H&E	Diagnosis of lung cancer subtypes	https://portal.gdc.cancer.gov/	939 cases	AUC: 0.8835	
Wang et al. (2019)	Hybrid	Gastric Cancer	H&E	Diagnosis of lymph node metastases	https://portal.gdc.cancer.gov/	884 cases	AUC: 0.9406	
Chen et al. (2021)	Hybrid	Non-small-cell Lung Cancer	H&E	Diagnosis of lymph node metastases	https://portal.gdc.cancer.gov/	3057 cases	AUC: 0.7288	
Chilente et al. (2020)	Hybrid	Prostate Cancer	H&E	Classification of glioma	Chik et al. (2013)	1065 cases	AUC: 0.906	
Shurns et al. (2021)	Hybrid	Gastrointestinal Cancers	H&E	Diagnosis of non-small-cell lung carcinoma subtypes	https://portal.gdc.cancer.gov/	316 cases	AUC: 0.771	
Li et al. (2021)	Hybrid	Cervical Disease	H&E	Diagnosis of patients with benign and malignant classification	in house	2485 cases	AUC: 0.738	
Myronenko et al. (2021)	Hybrid	Breast Cancer Renal Cell Carcinoma Non-Small-Cell Lung Cancer	H&E	Diagnosis of lymph node metastases	MSK breast cancer	9302 cases	AUC: 0.866	
Nak et al. (2020)	Clinical Studies	Breast Cancer	H&E	Diagnosis of lymph node metastases	http://thomashublab.org/data/	9304 cases	AUC: 0.895	
Tomita et al. (2019)	Clinical Studies	Esophagus Cancer	H&E	HER2 scoring (negative (0/1+), equivalent (2+) and positive (3+))	in house	939 cases	AUC: 0.973	
Skrode et al. (2020)	Clinical Studies	Colorectal Cancer	H&E	Prediction of normal and malignant tissues	in house	1105 cases	AUC: 0.870	
Kather et al. (2019)	Clinical Studies	Gastrointestinal Cancer	H&E	Prediction of patients with cellular disease or being healthy	Bejnordi et al. (2017b)	137 cases	AUC: 0.921	
Coudrey et al. (2018)	Clinical Studies	Lung Cancer	H&E	Detection of lymph node metastases	https://cancerimgingarchive.org/dataset/	139 cases	AUC: 0.982	
Bejnordi et al. (2017a)	Clinical Studies	Breast Cancer	H&E	Subtyping and the detection of lymph node metastases	https://cancerimgingarchive.org/dataset/	413 cases	AUC: 0.973	
Wessels et al. (2021)	Clinical Studies	Prostate Cancer	H&E	Classification of cancer tissue	https://cancerimgingarchive.org/dataset/	400 cases	AUC: 0.973	
Shurns et al. (2021)	Clinical Studies	Breast Cancer	H&E	Gastric cancer dataset	https://cancerimgingarchive.org/dataset/	400 cases	AUC: 0.973	
Li et al. (2021)	Clinical Studies	Esophagus Cancer	H&E	Prediction of tumor status	https://cancerimgingarchive.org/dataset/	884 cases	AUC: 0.973	
Skrode et al. (2020)	Clinical Studies	Colorectal Cancer	H&E	Determination of hormonal receptor status	https://cancerimgingarchive.org/dataset/	939 cases	AUC: 0.973	
Kather et al. (2019)	Clinical Studies	Gastrointestinal Cancer	H&E	Detection of cancerous and precancerous esophagus tissue	https://cancerimgingarchive.org/dataset/	1014 cases	AUC: 0.973	
Coudrey et al. (2018)	Clinical Studies	Lung Cancer	H&E	Prediction of colorectal cancer outcome	https://cancerimgingarchive.org/dataset/	180 cases	AUC: 0.973	
Amund et al. (2021)	Clinical Studies	Thyroid Cancer	H&E	Prediction of microsatellite instability	https://cancerimgingarchive.org/dataset/	2473 cases	AUC: 0.973	
Bejnordi et al. (2017a)	Clinical Studies	Breast Cancer	H&E	Classification of subtypes	https://cancerimgingarchive.org/dataset/	315 cases	AUC: 0.973	
Yang et al. (2022)	Clinical Studies	Prostate Cancer	H&E	Prediction of mutation from non-small-cell lung cancer	https://cancerimgingarchive.org/dataset/	300 cases	AUC: 0.973	
Li et al. (2021)	Clinical Studies	Breast Cancer	H&E	Detection of lymph node metastases	https://cancerimgingarchive.org/dataset/	378 cases	AUC: 0.973	
Saillard et al. (2020)	Clinical Studies	Hepatocellular Carcinoma	H&E	Prediction of BRAF mutation	Micromass (TH-THM17) dataset	36 cases	AUC: 0.92	
Vatimous et al. (2021)	Clinical Studies	Bladder Cancer	H&E	Prediction of HER2-positive breast cancer recurrence and metastasis	TCGA-ATCA dataset	444 cases	AUC: 0.77	
Woo et al. (2020)	Clinical Studies	Bladder Cancer	H&E	Predictive biomarker of risk	HR2-positive breast cancer dataset	127 cases	AUC: 0.76	
				Prediction of lymph node metastasis	The Cancer Genome Atlas (TCGA) dataset	123 cases	AUC: 0.94	
				Prediction of BRAF mutation	Breast cancer dataset	540 cases	AUC: 0.847	
				Prediction of survival after hepatochlear carcinoma resection	Discovery set	194 cases	AUC: 0.84	
				Identifying FGFR-activating mutations	The Cancer Genome Atlas (TCGA) dataset	328 cases	AUC: 0.88	
				Prediction of molecular subtypes	The Cancer Genome Atlas (TCGA) dataset	418 cases	AUC: 0.76	
				CC-CEMM cohort	Urothelial Bladder Cancer Dataset	407 cases	AUC: 0.89	
					CC-CEMM cohort	16 cases	AUC: 0.85	

### 3.2. Semi-Supervised Learning Paradigm

Semi-supervised learning is a branch of machine learning that combines both supervised and unsupervised learning tasks and improves model performance by exploiting the information associated between tasks (Zhu *et al.* 2005, Van *et al.* 2020). In semi-supervised learning, only a small amount of labeled data is generally available, and besides that, a large amount of unlabeled data can be available for network training. Consequently, the main goal of semi-supervised learning is how to use these unlabeled data to improve the performance of the model trained with limited labeled data. Scenarios of the semi-supervised learning paradigm are very common in the field of pathological image analysis, both in diagnostic tasks and in segmentation tasks. Due to the expensive and time-consuming fine-grained annotation, pathologists often can only provide a small number of precise annotations for supervised training of the models, while a large amount of unannotated data cannot be used. Training deep models with only these limited labeled data can easily lead to over-fitting, thus significantly harming the performance and generalization of the models. In the semi-supervised learning paradigm, a large number of unlabeled images can be used to assist in training and thus further improve the performance, generalization, and robustness of the models.

In the past two decades, numerous semi-supervised learning algorithms have been proposed and widely used in the fields of natural image processing and pathological image analysis. The representative approaches in the field of semi-supervised learning are divided into five categories, namely pseudo-labelling-based approach (Section 3.2.1), consistency-based approach (Section 3.2.2), graph-based approach (Section 3.2.3), unsupervised-preprocessing approach (Section 3.2.4), and other approaches (Section 3.2.5). We introduce these methods below, respectively. For each category, we first describe their fundamental principles and then elaborate on their representative studies in the field of pathological image analysis. For a systematic review of the assumptions, concepts and representative methods of semi-supervised learning in the field of natural images, we recommend the review by Van *et al.* 2020. Table 4 summarizes the detailed list of literatures in this section.

#### 3.2.1. Pseudo-labelling-based Approach

*Fundamental Principles* The pseudo-labeling-based approach is a classical and well-known semi-supervised method (Zhu *et al.* 2005), which mainly consists of two alternating processes, training and pseudo-labeling. Taking the classification problem as an example, in the training process, one or more classifiers are first trained in a supervised manner on the labeled data. The labeled data may be derived from the initial accurately labeled data or from the pseudo-labeled data from the previous iterations. In the pseudo-labeling process, all the unlabeled data are first predicted using the classifier trained in the previous process, and then the most confidently predicted portion of the data are selected for pseudo-labeling. Finally, these pseudo-labeled data are added to

the labeled data for the next iteration. This process is repeated until no data with high confidence are found or all data are labeled.

The pseudo-labeling-based methods are firstly applied to the field of natural image processing and typically contain self-training methods (Lee *et al.* 2013) and co-training methods (Blum *et al.* 1998, Zhou *et al.* 2005).

*Study in Pathological Image Analysis* In pathological image analysis, Singh *et al.* 2011 proposed a semi-supervised method of learning distance metrics from labeled data and performing label propagation for identifying the subtypes of nuclei, which was locally adaptive and could fully consider the heterogeneity of the data. Bulten *et al.* 2020 developed a deep learning system for Gleason scoring of prostate biopsies based on semi-supervised learning. They first trained the network on a small training dataset with pure Gleason scores, and then applied the trained network to other internal training datasets to set reference standards. Then, the labels were corrected and relabeled using reports from pathologists. Tolkach *et al.* 2020 used a pseudo-labeling-based semi-supervised strategy to train the CNN network to accomplish Gleason pattern classification. Jasiwal *et al.* 2019 proposed a semi-supervised method based on pseudo-labeling and entropy regularization for breast cancer pathological image classification. Shaw *et al.* 2020 extended the study of Yalniz *et al.* 2019 by proposing a semi-supervised teacher-student distillation method for the classification of colorectal cancer pathological images. Marini *et al.* 2021 proposed a deep pseudo-labeling-based semi-supervised learning method for strongly heterogeneous pathology data containing only a small number of local annotations. Their method consists of a high-volume teacher model and a small-volume student model, where the teacher model is automatically labeled with pseudo labels for the training of the student model. Cheng *et al.* 2020 proposed a semi-supervised learning framework based on a teacher-student model with similarity learning for the segmentation of breast cancer lesions containing a small number of annotations and noisy annotations.

### 3.2.2. Consistency-based Approach

*Fundamental Principles* The consistency-based semi-supervised learning approach is mainly based on the smoothing assumption. In the smoothing assumption, the prediction model should be robust to local perturbations within its input. This means that when we perturb the data points with a small amount of noise, the network's predictions for the perturbed data points and the clean original data points should be similar. In the implementation of deep neural networks, the consistency-based approach can be easily extended to a semi-supervised learning setup by directly adding unsupervised consistency loss functions to the original supervised loss functions. In the field of natural image processing, typical methods include  $\pi$ -model (Laine *et al.* 2016), Temporal Ensembling model (Laine *et al.* 2016), Mean Teachers (Tarvainen *et al.* 2017) and UDA (Xie *et al.* 2020).

*Study in Pathological Image Analysis* In pathological image analysis, Zhou *et al.* 2020 proposed a new Mean-teacher (MT) framework based on template-guided perturbation-sensitive sample mining. This framework consists of a teacher network and a student network. The teacher network is an integrated prediction network from K-times randomly augmented data, which is used to guide the student network to remain invariant to small perturbations at both feature and semantic levels. Su *et al.* 2019 proposed a novel global and local consistency loss and performed the nuclei classification task based on the Mean-Teacher framework.

### 3.2.3. Graph-based Approach

*Fundamental Principles* Methods of graph-based semi-supervised learning typically construct graphs to preserve the relationships of neighboring nodes, and use the graph transformations to simultaneously exploit information from labeled data and explore the underlying structure of unlabeled data. The key step of the graph-based semi-supervised learning methods is to construct a better graph to represent the original data structure. They usually define a graph on all data points (both labeled and unlabeled data points) and use weights to encode the similarity between pairs of the data points. In this way, the labeled information can be propagated through the graph to the unlabeled data points. For labeled data points, the predicted labels should match the true labels; similar data points defined by a similarity graph should have the same predictions. Graph-based semi-supervised methods are a relatively complex and long-developed field, and we recommend (Van *et al.* 2020, Chong *et al.* 2020) for a more thorough understanding.

*Study in Pathological Image Analysis* In pathological image analysis, Xu *et al.* 2016 proposed a new framework that combines a CNN with a semi-supervised regularization term. They first generated a hypothetical label for each unlabeled sample, then proposed a graph-based smoothing term for regularization. Su *et al.* 2015 proposed an active learning and graph-based semi-supervised learning method for interactive cell segmentation. Inspired by the Temporal Ensembling model (Laine *et al.* 2016), Shi *et al.* 2020 proposed a graph-based temporal ensembling model GTE. This method creates ensemble targets for both feature and label predictions for each training sample, and encourages the model to form consistent predictions under different perturbations to exploit the semantic information of unlabeled data and improve the robustness of the model to noisy labels.

### 3.2.4. Unsupervised-preprocessing-based Approach

*Fundamental Principles* Unlike the previous approaches, unsupervised preprocessing-based approaches are typically dedicated to the unsupervised feature extraction, clustering (cluster-then-label), or initialization of the parameters of the subsequent supervised learning process (pre-training) from a large amount of unlabeled data. The

most popular methods include autoencoders and their variants (Vincent *et al.* 2008, 2011). Clustering is another method that enables adequate learning of the overall data distribution, thus many semi-supervised learning algorithms (Goldberg *et al.* 2009, Demiriz *et al.* 1999, Dara *et al.* 2002) guide the subsequent classification process through clustering. The idea of the pre-training is to first pre-train a model using unsupervised methods with unlabeled data, and then use the parameters of this model as the initial parameters of the subsequent supervised training model, i.e., the subsequent supervised training is fine-tuned on the basis of these initial parameters. On this basis, the large number of unlabeled data can fully guide the subsequent classification models with limited labeled data thus improving the performance of semi-supervised learning (Erhan *et al.* 2010).

*Study in Pathological Image Analysis* In pathological image analysis, Peikari *et al.* 2018 proposed a cluster-then-label semi-supervised learning method for identifying high-density regions in the data space and then utilized these regions to help support vector machines find decision boundaries. Lu *et al.* 2019 proposed a semi-supervised method based on feature extraction and pre-training for the WSI-level breast cancer classification task, which is the first work that relies on self-supervised feature learning using contrastive predictive coding for weakly supervised histopathological image classification. Koohbanani *et al.* 2021 proposed a joint framework of self-supervised learning and semi-supervised learning for pathological images. They proposed three pathology-specific self-supervised tasks, magnification prediction, magnification jigsaw prediction and hematoxylin channel prediction, to learn high-level semantic information and domain invariant information in pathological images. Srinidhi *et al.* 2022 also proposed a framework that combines self-supervised learning with semi-supervised learning. They first proposed the resolution sequence prediction (RSP) self-supervised auxiliary task to pre-train the model through unlabeled data, and then they performed fine-tuning of the model on the labeled data. After that they used the trained model from the above two steps as the initial weights of the model for further semi-supervised training based on the teacher-student consistency framework.

### 3.2.5. Other Approaches

Among semi-supervised learning, there are many other approaches, such as the methods based on generative adversarial networks (GAN) (Goodfellow *et al.* 2014, 2016, Salimans *et al.* 2016, Odena *et al.* 2016, Dai *et al.* 2017), Manifold-based methods (Belkin *et al.* 2005, 2006, Weston *et al.* 2012, Rifai *et al.* 2011, 2011) and Association Learning based methods (Haeusser *et al.* 2017).

In pathological image analysis, Kapil *et al.* 2018 first used auxiliary classifier generative adversarial networks (AC-GAN) for the pathological image semi-supervised classification task and achieved favorable results. Cong *et al.* 2021 proposed to use a GAN-based semi-supervised learning method to accomplish the stain normalization problem for pathological images. Sparks *et al.* 2016 proposed a semi-supervised method

based on epidemic learning to accomplish a content-based histopathological image retrieval task. Li *et al.* 2018 developed an Expectation-Maximization (EM)-based semi-supervised method for the semantic segmentation task of radical prostatectomy histopathological images. Su *et al.* 2021 proposed a new semi-supervised method based on association learning for pathological image classification task inspired by Haeusser *et al.* 2017. Some studies (Foucart *et al.* 2019) have also attempted to analyze the weaknesses and effectiveness of semi-supervised, noisy learning and weak label learning based on deep learning for pathological image analysis.

### 3.3. Self-Supervised Learning Paradigm

Unlike the former two paradigms, the self-supervised learning paradigm does not perform the classification or segmentation of pathological images directly, but in a two-stage 'pre-training and fine-tuning' approach. Due to the small number of annotated pathological images, it is not enough to use these data to directly train the model. Therefore, the self-supervised learning paradigm aims to first learn effective feature representations from a large amount of unlabeled data, which is called the pre-training process. Afterwards, the feature representations learned in the self-supervised auxiliary tasks are used as the initial model weights to be transferred to train the downstream tasks using limited labeled data, which is called the fine-tuning process. In this way, good feature representations can effectively help the model to achieve good results even if it is trained with only a small amount of labeled data.

The process of pre-training, i.e., the learning process of good feature representations, is the key to self-supervised learning. Typically, self-supervised learning learns good feature representations by performing self-supervised auxiliary tasks. In a self-supervised auxiliary task, certain inherent properties of the unlabeled data are first used to generate supervised signals, and then the network is trained by these self-supervised signals. Different studies usually focus on designing different self-supervised auxiliary tasks to perform feature representation learning efficiently. According to the properties of the auxiliary tasks, existing self-supervised learning paradigms can be mainly classified into predictive self-supervised learning, generative self-supervised learning, and contrastive self-supervised learning. Predictive self-supervised learning learns good feature representations by constructing the auxiliary tasks as classification problems with unlabeled data; generative self-supervised learning learns good feature representations by reconstructing the input images; and contrastive self-supervised learning learns good feature representations by learning to distinguish between similar samples (positive samples) and dissimilar samples (negative samples). For a systematic review of self-supervised methods in the natural image domain and medical image domain, we recommend the reviews by Liu *et al.* 2021 and Shurab *et al.* 2021.

In this section, we provide a detailed review of the studies on self-supervised learning for pathological image analysis. Currently, some studies focus on proposing innovative self-supervised frameworks for pathological images (we call them study on novel self-

Table 4: List of literatures in the semi-supervised learning section.

Reference	Approach	Disease Type	Staining	Task		Dataset	Scale	Dataset Link	Performance
				3D fluorescence microscopy	Identifying nuclear phenotypes				
Singh et al. (2011)	Pseudo-labelling-based	Breast Cancer	H&E	Glasson grading	NoCell image dataset	984 images	Inhouse	Inhouse	Mean Accuracy: 0.8
Bulcen et al. (2020)	Pseudo-labelling-based	Prostate Cancer	H&E	Identification of prostate cancer tissue	Inhouse dataset	5759 biopsies from 1243 patients	Inhouse	Inhouse	AUC = 0.99
Tolbach et al. (2020)	Pseudo-labelling-based	Prostate Cancer	H&E	Glasson grading of prostate adenocarcinomas	The Cancer Genome Atlas (TCGA) dataset	1.67 million patches	http://zenodo.org/depot/3825933	http://zenodo.org/16.grand-challenge.org/Data/	Accuracy = 0.967
Jaiswal et al. (2019)	Pseudo-labelling-based	Breast Cancer	H&E	Detection of lymph node metastases	PatchCamelyon dataset	327680 patches	https://zenodo.org/record/1214464/YvyX3ZByw4	https://zenodo.org/16.grand-challenge.org/Data/	AUC = 0.9846
Shaw et al. (2020)	Pseudo-labelling-based	Colorectal Cancer	H&E	Classification of 9 categories of pathology patterns	Public dataset	100000 patches	https://zenodo.org/record/1214464/YvyX3ZByw4	https://zenodo.org/16.grand-challenge.org/Data/	Mean Accuracy = 0.943
Murini et al. (2021)	Pseudo-labelling-based	Prostate Cancer	H&E	Glasson grading	Tissue MicroArray dataset Zurich dataset	886 cases	Inhouse	Inhouse	$\kappa$ -score: 0.7645
Cheng et al. (2020)	Pseudo-labelling-based	Breast Cancer	H&E	Automated segmentation of cancerous regions	TCGA-PRAD dataset CAMELYON16 dataset	449 cases	http://camelyon16.grand-challenge.org/Data/	http://camelyon16.grand-challenge.org/Data/	$\kappa$ -score: 0.4529
Zhou et al. (2020)	Consistency-based	Prostate Cancer	H&E	Liquid-based Pap test specimen	TVGH TURP dataset	400 cases	Inhouse	Inhouse	Dice: 93.37
Su et al. (2019)	Consistency-based	-	H&E	Quantification of tumor cellularity	NoCell image dataset	71 cases	Inhouse	Inhouse	Dice: 77.24
Strindhi et al. (2022)	Consistency-based	Breast Cancer, Colorectal Cancer	H&E	Neuron segmentation	4339 cytoplasm	22462 nuclei	AfI: 73.45, MAP: 46.01	AfI: 73.45, MAP: 46.01	Mean Accuracy = 0.943
Xu et al. (2016)	Graph-based	-	H&E	Nuclei classification	McNeese dataset KU67 nucleus dataset	17516 nuclei	F1 score: 75.02 (5% labels)	F1 score: 75.02 (5% labels)	$\kappa$ -score: 0.7645
Su et al. (2015)	Graph-based	Lung Cancer	H&E	Detection of tumor metastasis	Breast PathQ dataset	2579 patches	TC: 0.876 (10% labels)	TC: 0.876 (10% labels)	TC: 0.876 (10% labels)
Shi, Su, Xing and Yang (2020)	Graph-based	Breast Cancer	H&E	Classification of tissue types	Camelyon16 dataset	399 WSIs	AUC: 0.855 (10% labels)	AUC: 0.855 (10% labels)	Accuracy: 0.982 (10% labels)
Pellati et al. (2018)	Unsupervised-preprocessing-based	Breast Cancer	H&E	Quantification of tumor cellularity	Kather multiclass dataset	100K patches	F1 score: 0.96 (40% labels)	F1 score: 0.96 (40% labels)	$\kappa$ -score: 0.86
Lu et al. (2019)	Unsupervised-preprocessing-based	Breast Cancer	H&E	Neuron segmentation	Neural morphology image dataset	2004 neuron regions	TC: 0.9813	TC: 0.9813	Accuracy: 0.895 (20% labels)
Koohkanian et al. (2021)	Unsupervised-preprocessing-based	Breast Cancer	H&E	Cell segmentation	Phase contrast microscopy image dataset	Multiple sequences of total 1040 frames	Accuracy: 0.905 (20% labels)	Accuracy: 0.905 (20% labels)	Accuracy: 0.895 (20% labels)
Koohkanian et al. (2021)	Unsupervised-preprocessing-based	Oral Squamous Cell Carcinoma	H&E	Predictions of subtypes	The Cancer Genome Atlas (TCGA) Pathology triaging	2694 patches	Inhouse	Inhouse	AUC: 0.86
Kopil et al. (2018)	GAN-based	Lung Cancer	H&E	Identifying different breast tissue regions	Nuclei figure classification dataset	1763 patches	Inhouse	Inhouse	AUC: 0.95
Cong et al. (2021)	GAN-based	Brain Cancer	H&E	Benign and malignant classification	BACH dataset	400 cases	BACH: Grand challenge on Breast Cancer histology images	BACH: Grand challenge on Breast Cancer histology images	Accuracy: 0.95
Sparks and Madabhushi (2016)	Manifold-learning-based	Prostate Cancer	H&E	Detection of tumor regions	Camelyon16 dataset	399 slides	http://camelyon16.grand-challenge.org/Data/	http://camelyon16.grand-challenge.org/Data/	AUC: 0.817 (1% labeled)
Li et al. (2018)	Expectation-Maximization-based	Breast Cancer, Colorectal Cancer	H&E	Prediction of metastases in the cervical lymph nodes	LN-M-OSCC dataset	217 slides	Inhouse	Inhouse	AUC: 0.806 (1% labeled)
Strindhi et al. (2022)	Unsupervised-preprocessing-based	-	H&E	Classification of tissue types	Kather multiclass dataset	100K patches	Kather et al. (2019)	Kather et al. (2019)	AUC: 0.983 (1% labeled)
				Detection of tumor metastasis	Breast PathQ dataset	2579 patches	Marel et al. (2019)	Marel et al. (2019)	TC: 0.876 (10% labels)
				Classification of tissue type	Camelyon16 dataset	399 WSIs	https://camelyon16.grand-challenge.org/Data/	Kather et al. (2019)	AUC: 0.855 (10% labels)
				Quantification of tumor cellularity	Kather multiclass dataset	100K patches	Kather et al. (2019)	Kather et al. (2019)	AUC: 0.982 (10% labels)
				Automated tumor proportion scoring	NSCLC needle biopsy dataset	270 slides	Inhouse	Inhouse	Ratio of the number of tumor positive cell pixels to the total number of tumor cell pixels: 0.94
				Ventana PD-L1 (SP263) assay	TCGA glioma cohort Breakalls database	22,229 images	Lin et al. (2020)	Lin et al. (2020)	Fl score: 0.937
				H&E	Stain normalisation	7,946 images	Spanhol et al. (2015)	Spanhol et al. (2015)	Fl score: 0.980
				H&E	Image retrieval	58 patients	Gervich et al. (2015)	Gervich et al. (2015)	Fl score: 0.914
				H&E	Semantic segmentation	135 fully annotated and 1800 weakly annotated tiles	Arrojo et al. (2017)	Arrojo et al. (2017)	Fl score: 0.495
				H&E	Classification of cancerous and non-cancerous slides	25 images	Aresta et al. (2019)	Aresta et al. (2019)	Fl score: 0.75
				H&E	Brahmsing 2015 challenge dataset	400 images			Fl score: 0.77

supervised frameworks), while others attempt to apply existing self-supervised learning methods to pathological image analysis (we call them study on application of self-supervised frameworks). We introduce studies on novel self-supervised frameworks in Section 3.3.1, where we focus on predictive self-supervised learning and its state-of-the-art approaches in pathological image analysis in Section 3.3.1, generative self-supervised learning in Section 3.3.1, contrastive self-supervised learning in Section 3.3.1, and hybrid self-supervised learning in Section 3.3.1. We introduce the study on application of self-supervised frameworks in Section 3.3.2. Table 5 summarizes a detailed list of literatures in this section.

### 3.3.1. Study on Novel Self-supervised Frameworks

#### *Predictive Self-supervised Learning Approach*

*Fundamental Principles* Predictive self-supervised learning learns good feature representations by constructing the auxiliary tasks as classification problems with unlabeled data, and the class labels for classification are constructed from the unlabeled data itself. Currently, predictive self-supervised auxiliary tasks widely applied in natural image processing are relative position prediction (Doersch *et al.* 2015), solving Jigsaw puzzles (Noroozi *et al.* 2016), and rotation angle prediction (Gidaris *et al.* 2018), etc.

*Study in Pathological Image Analysis* In the field of pathological image processing, Sahasrabudhe *et al.* 2020 proposed the auxiliary task of predicting patch magnification for cell nuclei segmentation. Their main idea is that given WSIs of different magnification classes (e.g., 5 $\times$ , 10 $\times$ , 20 $\times$ ), they first obtained patches of different magnifications from them and then predicted the magnification class of those patches by examining the size and texture of the cell nuclei in the patches. Srinidhi *et al.* 2022 proposed the resolution sequence prediction (RSP) auxiliary task. First they used patches with different magnifications to construct different combinations of resolution sequences, and then trained the network to predict the order of the resolution sequences. Koohbanani *et al.* 2021 proposed magnification prediction and solving magnification puzzles auxiliary tasks for pathological images. They first trained the network to accurately predict the magnification category, and then trained the network to predict the order of the patches with different magnifications.

#### *Generative Self-supervised Learning Approach*

*Fundamental Principles* Generative self-supervised learning learns good feature representations by reconstructing the input images. They argue that the image itself is a useful self-supervised information and that the network can learn the potential feature representations of the generated image during the image reconstruction process. In natural image processing, autoencoders (Goodfellow *et al.* 2016) are representative of

early work on generative self-supervised feature representation learning. Later, denoising autoencoders (Vincent *et al.* 2008) enhanced the feature representation capability of the model by introducing noise. Subsequently, researchers proposed a series of reconstructive self-supervised auxiliary tasks, including inpainting (Pathak *et al.* 2016), colorization (Zhang *et al.* 2016), patch shuffling and restoration (Chen *et al.* 2019, Zhou *et al.* 2021) to further enhance the feature representation capability of the network and achieved promising results. On the other hand, a series of GAN-based models (e.g., DCGAN 2015, BiGAN 2016) have also been used to perform self-supervised representation learning. In the latest self-supervised studies on natural images, a series (e.g., BEiT 2021, MAE 2021, PeCo 2021, etc.) of self-supervised studies based on masked image blocks and reconstruction using Transformer achieved the highest performance, which is expected to start a new wave of research on reconstruction-based self-supervised representation learning.

*Study in Pathological Image Analysis* In pathological image analysis, Muhammad *et al.* 2019 proposed a new deep convolutional autoencoder-based clustering model to learn the feature representations of pathological images. Mahapatra *et al.* 2020 incorporated semantic information into a GAN-based generative model for self-supervised feature representation learning and used it for the stain normalization task of pathological images. Quiros *et al.* 2019, 2021 designed GANs for pathological images to extract key feature representations of tissues. Boyd *et al.* 2021 proposed a new generative auxiliary task which performs representation learning by extending the view of image patches. Hou *et al.* 2019 proposed a sparse convolutional autoencoder (CAE) for simultaneous nuclei detection and feature extraction in histopathological images. Koohbanani *et al.* 2021 proposed the hematoxylin channel prediction auxiliary task, where they used hematoxylin and eosin (H&E) stained images to predict the hematoxylin channel pixel by pixel.

### *Contrastive Self-supervised Learning Approach*

*Fundamental Principles* The contrastive self-supervised approach is one of the most popular self-supervised paradigms, which focuses on learning good feature representations by encouraging the model to learn to distinguish between similar samples (positive samples) and dissimilar samples (negative samples).

Contrast predictive coding (CPC) (Van *et al.* 2018) is an early contrastive self-supervised method applied to natural image processing whose goal is to maximize the mutual information between patches (positive samples) from the same image and minimize the mutual information between patches (negative samples) from different images within a mini-batch. Typical subsequent studies have been devoted to constructing negative samples. MoCo (He *et al.* 2020) is a momentum-based contrastive self-supervised framework, which is mainly based on the ideas of dynamic dictionary-lookup and queues. SimCLR (Chen *et al.* 2020) is a simple contrastive learning

framework that aims to maximize the cosine similarity between two augmented views of the same image (positive samples) and minimize the similarity between different images in a minibatch (negative samples).

These methods rely heavily on a large number of negative samples since only positive samples will easily lead to model degeneration, i.e., mapping the features of all samples to an identical vector. However, recent studies have shown that negative samples are not necessary. Caron *et al.* 2020 introduced clustering into contrastive learning, thus eliminating the need for negative samples. Chen *et al.* 2021 explored stop-gradient operation applied to siamese networks without the need for a large number of negative samples. Grill *et al.* 2020, Caron *et al.* 2021 proposed a self-supervised learning model based on a teacher-student knowledge distillation framework that achieves state-of-the-art performance without any negative samples.

*Study in Pathological Image Analysis* In pathological image analysis, Xie *et al.* 2020 employed patches from different magnifications as positive samples and patches from different magnifications as negative samples and constructed scale-wise triplet loss to perform contrastive learning for the nuclei segmentation. Chhipa *et al.* 2022 proposed Magnification Prior Contrastive Similarity (MPCS) to construct contrastive loss. Xu *et al.* 2020 proposed a self-supervised Deformation Representation Learning (DRL) framework to learn semantic features from unlabeled pathological images. They used mutual information to train the network to distinguish original histopathological images from those deformed in local structure, while consistent global contextual information was maintained using noise contrastive estimation (NCE). Wang *et al.* 2021 proposed Transpath based on the BYOL framework 2020. They first collected the current largest histopathological image dataset for self-supervised pre-training, which includes about 2.7 million images from 32529 WSIs. Then they proposed a hybrid framework combining CNN and Transformer to extract both local structural features and global contextual features, and proposed a TAE module to further enhance the feature extraction capability.

*Hybrid Self-supervised Learning Approach* Many studies have also presented hybrid self-supervised methods for pathological images. Abbet *et al.* 2020 proposed a combination of generative and contrastive self-supervised representation learning method for pathological images. They first applied colorization as a generative auxiliary task. Then, they constructed the contrastive loss using spatially neighboring patches as positive samples and distant patches as negative samples. Yang *et al.* 2021 also proposed a self-supervised representation method combining generative and contrastive approaches for pathological images. They first proposed a generative-based self-supervised task called cross-stain prediction, in which they defined two encoders and decoders to predict the E-channel and H-channel, respectively, and then they used the encoders trained in the previous task to perform further contrastive training.

### 3.3.2. Study on Applications of Self-supervised Frameworks

In addition to studies that aim to propose innovative self-supervised frameworks for pathological images, more studies have attempted to apply existing self-supervised learning methods to various pathological image analysis tasks. Chen *et al.* 2020 proposed an end-to-end multimodal fusion framework for histopathological images and genomic data for survival prognosis prediction, in which they used contrastive predictive coding (CPC) pre-trained self-supervised features for initialization of the network model. Ciga *et al.* 2022 showed through extensive experiments that using self-supervised pre-training methods can yield better features to improve performance on several downstream tasks. They found that the success of contrastive self-supervised pre-training methods depended heavily on the diversity of the unlabeled training set rather than the number of images. On the other hand, positive and negative samples that are visually significantly different facilitate contrastive self-supervised learning, while positive and negative sample that contain only minor differences but are generally similar (e.g., normal patches versus patches containing only a small percentage of tumor regions) are not conducive to contrastive learning. However, this is uncommon in natural images, so it is particularly important to design targeted self-supervised tasks for the characteristics of pathological images. Tellez *et al.* 2019 used the variational autoencoder 2013, contrastive learning 2016 and BiGAN 2016 for the compression of gigapixel pathological images and evaluated the performance on a synthetic dataset and two public histopathology datasets, respectively, achieving promising results. Stacke *et al.* 2021 investigated how SimCLR 2020 could be extended for pathological images to learn useful feature representations. They systematically compared the differences between ImageNet data and histopathology data and how this affected the goals of self-supervised learning, and pointed out the impact that designing for different self-supervised goals would have on the results. Chen *et al.* 2022 comprehensively compared the performance of ImageNet pre-trained features, SimCLR pre-trained features, and DINO 2021 pre-trained features in weakly supervised classification and fully supervised classification tasks for histopathological images. They found that the DINO-based knowledge distillation framework could better learn effective and interpretable features in pathological images.

Saillard *et al.* 2021 and Dehaene *et al.* 2020 used the MoCo V2 2020 self-supervised learning method to train pathological images and the experimental results showed that the results using the self-supervised pre-trained features were consistently better than those using features pre-trained on ImageNet under the same conditions. Lu *et al.* 2019, Zhao *et al.* 2020, and Li *et al.* 2021 used contrastive predictive coding (CPC) 2018, VAE-GAN 2016, and SimCLR 2020 self-supervised pre-trained features for weakly supervised WSI classification, respectively, and achieved the current state-of-the-art performance. Koohbanani *et al.* 2021 developed a semi-supervised learning framework facilitated by self-supervised learning with a multi-task learning approach for training, i.e., training with a small amount of labeled data as the main task and self-supervised tasks as auxiliary tasks. In their study, they also compared the effectiveness of various

commonly used pathology-agnostic self-supervised auxiliary tasks (including rotation, flipping, auto-encoder, real/fake prediction, domain prediction, etc.) to facilitate semi-supervised learning. Srinidhi *et al.* 2022 also attempted to use self-supervised pre-trained features to enhance semi-supervised learning. They first proposed the resolution sequence prediction (RSP) self-supervised auxiliary task to pre-train the model through unlabeled data, and then they fine-tuned the model on the labeled data. After that, they used the trained model from the above two steps as the initial weights of the model for further semi-supervised training based on the teacher-student consistency framework.

In addition, self-supervised learning has been used for a variety of other pathological tasks, such as pathological image retrieval (Shi *et al.* 2018, Yang *et al.* 2020), active learning (Zheng *et al.* 2019), and molecular signature prediction (Ding *et al.* 2020, Fu *et al.* 2020, Kather *et al.* 2020), etc.

## 4. Discussion and Future Trends

### 4.1. For Weakly Supervised Learning Paradigm

The two main goals of WSI analysis using the weakly supervised learning paradigm are global slide classification, which aims to accurately predict the labels of each WSI, and positive patch localization, which aims to accurately predict the labels of each positive patch in the positive bags. Among above two tasks, the former can be used for rapid automatic diagnosis of clinical pathology slides, such as early clinical screening, and the latter can be used for precise localization of tumor cells, as well as interpretable analysis of clinical diagnosis by deep learning networks. Based on the diagnostic results obtained from the whole slides, pathologists are often more interested in the precise location of tumor cells, the cell morphology and other microstructures for further analysis and corroboration. On the other hand, pathologists also expect new knowledge from the diagnosis of the deep neural networks, such as discovering new pathological patterns and structures, etc. A few current algorithms can perform the task of global slide classification well, but the task of positive patch localization is another challenge for most algorithms. A primary reason is that the loss functions of most bag-based deep MIL algorithms are defined only at the bag-level, and although mechanisms such as attention (Ilse *et al.* 2018) can be used to measure the contribution of each instance to the bag-level classification, the network does not have enough motivation to classify all instances accurately (Shi *et al.* 2020, Qu *et al.* 2022). On the other hand, instance-based methods and hybrid methods, although defining instance-level classifiers, usually face a high risk of errors in pseudo-labeling or key instance selection. Therefore, it is a new challenge for the weakly supervised learning paradigm to further improve the ability to classify instances while obtaining a better slide-level diagnosis.

Further, with the emergence of the methods of the weakly supervised segmentation in the natural image processing field (Ru *et al.* 2022, Xu *et al.* 2022, Pan *et al.* 2022, Lee *et al.* 2021, Chen *et al.* 2022), a new challenging direction for WSI analysis is to perform

Table 5: List of literatures in the self-supervised learning section.

Reference	Approach	Disease Type	Staining	Dataset	Dataset Scale	Dataset Link	Self-supervised Method	Downstream Task	Downstream Performance
Sahasrabudhe et al. (2020)	Predictive	-	H&E	MoNuSeg database	1,125,737 tiles	Kumar et al. (2017)	Identification of the magnification levels for tiles	Nuclei segmentation	AUJ: 0.5354, AHD: 7.7502, Dice: 0.7477
Srinidhi et al. (2022)	Predictive	Breast Cancer, Colorectal Cancer	H&E	BreastPathQ dataset Camelyon16 dataset Kather multiclass dataset	2579 patches 399 WSIs 100K patches	Martel et al. (2019) <a href="https://camelyon16.grand-challenge.org/Data/">https://camelyon16.grand-challenge.org/Data/</a> Kather et al. (2019)	Predicting the resolution sequences	Detection of tumor metastasis Classification of tissue types Quantification of tumor cellularity	TC: 0.876 (10% labels) AUC: 0.855 (10% labels) Accuracy: 0.982 (10% labels)
Koohbanani et al. (2021)	Predictive	Breast Cancer oral Squamous Cell Carcinoma Colorectal Cancer	H&E	Camelyon16 dataset LNM-OSCC dataset Kather multiclass dataset	399 slides 217 slides 100K patches	<a href="https://camelyon16.grand-challenge.org/Data/">https://camelyon16.grand-challenge.org/Data/</a> Ihhouse Kather et al. (2019)	Magnification prediction and solving magnification puzzles	Detection of tumor regions Prediction of metastases in the cervical lymph nodes Classification of tissue types	AUC: 0.817 (1% labeled) AUC: 0.806 (1% labeled) AUC: 0.903 (1% labeled)
Muhammad et al. (2019)	Generative	Cholangiocarcinoma	H&E	Intrahepatic cholangiocarcinoma (IC) dataset	240 patients	Ihhouse	Deep clustering convolutional autoencoder	Subtyping of cholangiocarcinoma	CH: 3893/5 clusters and 4314 (clustering weight = 0.2)
Malapatra et al. (2020)	Generative	Breast Cancer	H&E	CAMELYON16 dataset	100,000 patches	<a href="https://camelyon16.grand-challenge.org/Data/">https://camelyon16.grand-challenge.org/Data/</a>	Using pre-trained networks for semantic guidance	Stain normalization	Average AUC: 0.9320
Quiros et al. (2019)	Generative	Colorectal Cancer	H&E	National Center for Tumor diseases (NCT) dataset	86 slides	<a href="https://zenodo.org/record/1214456#.Yvzd-nZBxhE">https://zenodo.org/record/1214456#.Yvzd-nZBxhE</a>	Using Generative Adversarial Networks (GANs) to capture key tissue features and structure information	Count of cancer, lymphocytes, or stromal cells	FID: 16.65
Quiros et al. (2021)	Generative	Breast Cancer	H&E	Netherlands Cancer Institute (NKI) dataset and Vancouver General Hospital (VGH) dataset	576 tissue micro-arrays (TMAs)	Beck et al. (2011)			FID: 32.05
Quiros et al. (2021)	Generative	Breast Cancer	H&E	Netherlands Cancer Institute (NKL Netherlands) and Vancouver General Hospital (VGH, Canada) cohorts	Total of 576 patients	Beck et al. (2011)	Presenting an adversarial learning model to extract feature representations of cancer tissue	Classifying tissue types and predicting the presence of tumor in Whole Slide Images (WSIs) using multiple instance learning (MIL)	AUC: 0.97 and Accuracy: 0.85, AUC: 0.98 and Accuracy: 0.94
Koohbanani et al. (2021)	Generative	Colon cancer	H&E	National Center for Tumor diseases (NCT, Germany) dataset	100K tissue tiles	<a href="https://zenodo.org/record/1214456#.Yvzd-nZBxhE">https://zenodo.org/record/1214456#.Yvzd-nZBxhE</a>			
Koohbanani et al. (2021)	Generative	Lung Cancer	H&E	TCGA LUAD, LUSC dataset	1184 patients	<a href="http://portal.gdc.cancer.gov">http://portal.gdc.cancer.gov</a>			
Boyd et al. (2021)	Generative	Breast Cancer	H&E	CAMELYON17 dataset	500 slides	<a href="https://camelyon16.grand-challenge.org/Data/">https://camelyon16.grand-challenge.org/Data/</a>	Visual field expansion	Binary classification of tiles into metastatic and non-metastatic classes	Accuracy: 0.8569
Boyd et al. (2021)	Generative	Colorectal Cancer	H&E	CRC benchmark dataset	100K image tiles	<a href="https://doi.org/10.5281/zenodo.1214456">https://doi.org/10.5281/zenodo.1214456</a>		Classification of tiles into the 9 tissue types	Accuracy: 0.8511
Koohbanani et al. (2021)	Generative	Breast Cancer Oral Squamous Cell Carcinoma Colorectal Cancer	H&E	Camelyon16 dataset LNM-OSCC dataset Kather multiclass dataset	399 slides 217 slides 100K patches	<a href="https://camelyon16.grand-challenge.org/Data/">https://camelyon16.grand-challenge.org/Data/</a> Ihhouse Kather et al. (2019)	Hematoxylin channel prediction auxiliary task	Detection of tumor regions Prediction of metastases in the cervical lymph nodes Classification of tissue types	AUC: 0.817 (1% labeled) AUC: 0.806 (1% labeled) AUC: 0.903 (1% labeled)
Hou et al. (2019)	Generative	-	H&E	Self-collected lymphocyte classification dataset	1785 images	Ihhouse			Nucleus Classification: 0.7856 Lymphocyte Classification: AUC 0.8788
Xie, Chen, Li and Zheng (2020)	Contrastive	-	H&E	MoNuSeg dataset	41 images	Naylor et al. (2018)	Scale-wise triplet learning and count ranking	Nuclei segmentation	AUJ: 0.7063
Chhipa et al. (2022)	Contrastive	Breast Cancer	H&E	BreakHis dataset	7909 images	Spanhol et al. (2015)	Magnification point contrastive similarity	Classifying histopathological images	Mean Accuracy: 0.9233
Xu et al. (2020)	Contrastive	Breast Cancer Colon Cancer	H&E	MICCAI 2015 Gland Segmentation Challenge (GLaS) dataset PatchCamelyon (PCam) image classification dataset	165 images 327,680 patches	Sriramkunwattana et al. (2017) <a href="https://wiki.cancerimagingarchive.net/pages/viewpage.action?pageId=20644646">https://wiki.cancerimagingarchive.net/pages/viewpage.action?pageId=20644646</a>	Sparse Convolutional Autoencoder (CAE)	Gland segmentation Deformation representation learning	Nucleus detection: F-measure: 0.8345 Lymphocyte classification: AUC 0.7856 Nucleus segmentation: DICE: 0.8362
Wang et al. (2021)	Contrastive	Liver, Renal, Colorectal, Prostatic, Pancreatic, and Cholangio-Breast Cancers	H&E	Multiple histopathological image datasets including MHIST, NCT-CRC-HE, PatchCamelyon dataset	2.7 million images	<a href="https://github.com/Xiyue-Wang/TransPath">https://github.com/Xiyue-Wang/TransPath</a>	Contrastive learning like BYOL, Bootstrap your own latest: a new approach to self-supervised learning	Histopathological image classification tasks	F1-score: 0.8993, 0.9582, 0.5893 on MHIST, NCT-CRC-HE, PatchCamelyon dataset
Abbet et al. (2020)	Generative + Contrastive	Colorectal Cancer	H&E	Clinicopathological dataset	660 WSIs	Ihhouse	Colorization, Image reconstruction and Contrastive learning	Survival analysis	C-Index: 0.6943
Yang et al. (2021)	Generative + Contrastive	Colorectal Cancer	H&E	NCTCRC-HE-100K dataset	100K images	<a href="https://zenodo.org/record/1214456#.Yvzd-nZBxhE">https://zenodo.org/record/1214456#.Yvzd-nZBxhE</a>	Cross-stain prediction, Contrastive training	Nine-class classification of histopathological images	Accuracy of eight-class classification with only 1,000 labeled data: 0.915
Chen, Lu and Mahmood (2020)	Application	Glioma and Cell Carcinoma	H&E	The Cancer Genome Atlas (TCGA) dataset	1505 images	<a href="http://portal.gdc.cancer.gov">http://portal.gdc.cancer.gov</a>	Contrastive predictive coding (CPC)	Survival prognosis prediction	C-Index: 0.826
Ciga et al. (2022)	Application	Multiple Types	H&E	Out of the total 57 datasets from various institutions	A large number of images	<a href="https://github.com/cancigc-self-supervised-histopathology">https://github.com/cancigc-self-supervised-histopathology</a>	Contrastive learning	Classification, Regression, and Segmentation	Multiple results
Tellez et al. (2019)	Application	Breast Cancer	H&E	Camelyon16 dataset TUPAC16 dataset	400 WSIs 492 WSIs	<a href="https://camelyon16.grand-challenge.org/Data/">https://camelyon16.grand-challenge.org/Data/</a> Veta et al. (2019)	Variational autoencoder, Contrastive learning and BiGAN	Predicting the presence of metastasis	AUC: 0.725 Spearman correlation: 0.522
Stacke et al. (2021)	Application	Multiple Types	H&E	Camelyon16 dataset AIDA-LNSK dataset Multidata (samples from 60 publicly available datasets)	400 slides 96 slides A large number of images	<a href="https://github.com/k-stacke/ssl-pathology">https://github.com/k-stacke/ssl-pathology</a>	Contrastive learning	Binary tumor classification	Multiple results
Chen and Krishnan (2022)	Application	Colorectal Cancer Breast Cancer	H&E	CRC-100K dataset BreastPathQ dataset	100K images 2766 patches	Kather et al. (2016) Petrick et al. (2021)	Contrastive learning	Weakly-supervised cancer subtyping	AUC: 0.886
Saillard et al. (2021)	Application	Colorectal Cancer Gastric Cancer	H&E	TCGA-CRC dataset TCGA-Gastric dataset	55 patients 375 patients	<a href="http://portal.gdc.cancer.gov">http://portal.gdc.cancer.gov</a>	Contrastive learning	Patch-level tissue phenotyping Microsatellite instability	AUC: 0.987 AUC: 0.92 AUC: 0.83
Dehaene et al. (2020)	Application	Colorectal Cancer Breast Cancer	H&E	Camelyon16 dataset TCGA-COAD dataset	400 slides 461 slides	<a href="https://camelyon16.grand-challenge.org/Data/">https://camelyon16.grand-challenge.org/Data/</a> Guimay et al. (2015)	Contrastive learning	Predicting lymph node metastasis in Breast Cancer Colorectal Cancer subtyping	AUC: 0.882 (CMS1) and AUC: 0.829 (CMS3)
Lu et al. (2019)	Application	Breast Cancer	H&E	BACH dataset	400 cases	Aresta et al. (2019)	Contrastive predictive coding (CPC)	Classification and localization of clinically relevant histopathological classes	Accuracy: 0.95
Zhao et al. (2020)	Application	Colon Adenocarcinoma	H&E	The Cancer Genome Atlas (TCGA) dataset	425 patients	<a href="http://portal.gdc.cancer.gov">http://portal.gdc.cancer.gov</a>	Variational Auto Encoder and Generative Adversarial Network (VAE-GAN)	Predicting lymph node metastasis	Accuracy: 0.6761
Li, Li and Eliceiri (2021)	Application	Breast Cancer Lung Cancer	H&E	Camelyon16 dataset TCGA lung cancer dataset	400 cases 1054 cases	<a href="https://camelyon16.grand-challenge.org/Data/">https://camelyon16.grand-challenge.org/Data/</a> <a href="https://www.cancer.gov/about-ncl/organization/crc/research/structural-genomics/tcga">https://www.cancer.gov/about-ncl/organization/crc/research/structural-genomics/tcga</a>	Contrastive learning	Detection of lymph node metastases Diagnosis of lung cancer subtypes	Accuracy: 0.8992 Accuracy: 0.9571
Koohbanani et al. (2021)	Application	Breast Cancer Oral Squamous Cell Carcinoma Colorectal Cancer	H&E	Camelyon16 dataset LNM-OSCC dataset Kather multiclass dataset	399 slides 217 slides 100K patches	<a href="https://camelyon16.grand-challenge.org/Data/">https://camelyon16.grand-challenge.org/Data/</a> Martel et al. (2019) Kather et al. (2019)	Magnification prediction, JIG-Mag prediction and Hematoxylin channel prediction	Detection of tumor regions Prediction of metastases in the cervical lymph nodes Classification of tissue types	AUC: 0.817 (1% labeled) AUC: 0.806 (1% labeled) AUC: 0.903 (1% labeled)
Srinidhi et al. (2022)	Application	Breast Cancer, Colorectal Cancer	H&E	BreastPathQ dataset Camelyon16 dataset Kather multiclass dataset	2579 patches 399 WSIs 100K patches	<a href="https://camelyon16.grand-challenge.org/Data/">https://camelyon16.grand-challenge.org/Data/</a> Kather et al. (2019)	Resolution sequence prediction	Detection of tumor metastasis Classification of tissue types Quantification of tumor cellularity	TC: 0.876 (10% labels) AUC: 0.855 (10% labels) ACC: 0.982 (10% labels)
Zheng et al. (2019)	Application	Colon Cancer	H&E	MICCAI 2015 Gland Segmentation Challenge (GLaS) dataset Fungus dataset	165 images 84 images	Sriramkunwattana et al. (2017) Zhang et al. (2017)	Variational Auto Encoder (VAE)	Active learning in biomedical image segmentation	F1 score: 0.909, 0.9252 (30% labeled)

pixel-level semantic segmentation of the entire WSI based on weak or sparse labels. The task of the positive patch localization, which described in the previous section is still based on the classification of patches, and it is a more challenging task to further obtain pixel-level segmentation results based on the weak labels. A few current studies (Xu *et al.* 2019, Qu *et al.* 2020, Belharbi *et al.* 2021, Lerousseau *et al.* 2020) have made attempts in this new direction, but they still face many problems such as lack of details and precision on the segmentation results. Overall, for the weakly supervised learning paradigm, how to obtain the most detailed segmentation results as possible with weak labels is another promising study direction.

Another urgent need is the publicly available datasets with fine-grained annotations at the WSI level. As we all know, the scarcity of the publicly available pathological image datasets is an important factor hindering the development of the field. In recent years, we are grateful for the support of large public pathology datasets such as TCGA (2019), but public pathology datasets with fine-grained annotations are still in short supply for deeper research. To our knowledge, the large public dataset with detailed annotation at the WSI level is merely CAMELYON (Bejnordi *et al.* 2017a). We should encourage an individual or organization to provide more WSI-level public datasets with detailed annotations to promote the development of this study field.

#### 4.2. For Semi-Supervised Learning Paradigm

For semi-supervised learning paradigm, a new study direction is the combination with active learning, the purpose of which is to use the most effective labeled data to obtain the highest performance. Active learning aims to find the most valuable samples in the unlabeled dataset to be annotated through iterative interactions with experts, which allows to further exploit the effects of semi-supervised learning. There are already a lot of studies on pathological image analysis with the help of active learning (Zheng *et al.* 2019, Yang *et al.* 2017) or combination with semi-supervised learning and active learning (Su *et al.* 2015, Parag *et al.* 2014).

Another challenge is the effect that noisy data and domain variation have on the performance of semi-supervised learning algorithms. In the field of computational pathology, noisy annotations are very common, because the instance features of pathological images are very complex and variable, and their sizes are so huge that doctors are likely to suffer from missing and mislabeling during annotation. When performing multicenter validation, significant staining variation between the slides from different centers is also very common as there is no uniform standard for staining pathological images among different centers. Both the noisy labels and the domain variation are powerful factors that affect the performance of semi-supervised learning in real-world scenarios. Recent studies (Koohbanani *et al.* 2021, Cheng *et al.* 2020, Shi *et al.* 2020, Foucart *et al.* 2019, Marini *et al.* 2021) have made efforts on these two problems, and more studies in this field are expected.

#### 4.3. For Self-Supervised Learning Paradigm

For self-supervised learning paradigm, although current relevant studies in the field of natural images are developing rapidly, the direct applications of these methods to pathological images will be hindered by the strong domain discrepancy (Ciga *et al.* 2022, Koohbanani *et al.* 2021). Therefore, how to design more effective self-supervised auxiliary tasks for pathological images is a promising direction.

On the other hand, self-supervised learning has been promoting the development of weakly supervised learning and semi-supervised learning in pathological image analysis. As we all know, it is difficult for a network to learn effective feature representations with very limited annotations. In contrast, self-supervised learning is very suitable for learning effective feature representations from a lot of unlabeled data. Therefore, it will be a popular way to combine the features extracted by self-supervised pre-training with the weakly supervised or semi-supervised downstream tasks in the future. On the one hand, the efficient feature representations obtained from self-supervised pre-training will greatly improve the efficiency of weakly supervised learning and semi-supervised learning, and on the other hand, weakly supervised learning or semi-supervised learning will fully release the new potential of self-supervised learning in the field of computational pathology.

#### 4.4. Limitations

This review also contains several limitations. First, due to space limitations, this review does not include more clinical studies. We focus more on top technical conferences and journals and do not include more excellent papers published in clinical journals. For more systematic reviews of clinical studies, see (Cifci *et al.* 2022) and (Kleppe *et al.* 2021) for details. In addition, since there are so many technical studies on artificial intelligence applied to computational pathology, it is difficult to summarize them all, and due to space limitations, we have tried to include as many recent articles as possible, while some of them have not been included.

### 5. Conclusion

In this review, we provide a systematic summary and generalization of recent studies on weakly supervised learning, semi-supervised learning, and self-supervised learning in the field of computational pathology from the theoretical and methodological perspectives. On this basis, we also present targeted solutions to some current difficulties and shortcomings in this field, and illustrate its future trends. Through a survey of over 130 papers, we find that the field of computational pathology is marching at high speed into a new era, which is automatic diagnosis and analysis with fewer annotation needs, wider application scope, and higher prediction accuracy.

## Acknowledgments

This work was supported by National Natural Science Foundation of China under Grant 82072021.

## References

Abbet, C., Zlobec, I., Bozorgtabar, B. and Thiran, J.-P. (2020). Divide-and-rule: self-supervised learning for survival analysis in colorectal cancer, *International Conference on Medical Image Computing and Computer-Assisted Intervention*, Springer, pp. 480–489.

Anand, D., Yashashwi, K., Kumar, N., Rane, S., Gann, P. H. and Sethi, A. (2021). Weakly supervised learning on unannotated h&e-stained slides predicts braf mutation in thyroid cancer with high accuracy, *The Journal of Pathology* **255**(3): 232–242.

Araújo, T., Aresta, G., Castro, E., Rouco, J., Aguiar, P., Eloy, C., Polónia, A. and Campilho, A. (2017). Classification of breast cancer histology images using convolutional neural networks, *PloS One* **12**(6): e0177544.

Aresta, G., Araújo, T., Kwok, S., Chennamsetty, S. S., Safwan, M., Alex, V., Marami, B., Prastawa, M., Chan, M., Donovan, M. et al. (2019). Bach: Grand challenge on breast cancer histology images, *Medical Image Analysis* **56**: 122–139.

Bao, H., Dong, L. and Wei, F. (2021). Beit: Bert pre-training of image transformers, *arXiv preprint arXiv:2106.08254*.

Basavanhally, A., Ganesan, S., Feldman, M., Shih, N., Mies, C., Tomaszewski, J. and Madabhushi, A. (2013). Multi-field-of-view framework for distinguishing tumor grade in er+ breast cancer from entire histopathology slides, *IEEE Transactions on Biomedical Engineering* **60**(8): 2089–2099.

Beck, A. H., Sangoi, A. R., Leung, S., Marinelli, R. J., Nielsen, T. O., Van De Vijver, M. J., West, R. B., Van De Rijn, M. and Koller, D. (2011). Systematic analysis of breast cancer morphology uncovers stromal features associated with survival, *Science Translational Medicine* **3**(108): 108ra113–108ra113.

Bejnordi, B. E., Veta, M., Van Diest, P. J., Van Ginneken, B., Karssemeijer, N., Litjens, G., Van Der Laak, J. A., Hermsen, M., Manson, Q. F., Balkenhol, M. et al. (2017a). Diagnostic assessment of deep learning algorithms for detection of lymph node metastases in women with breast cancer, *Jama* **318**(22): 2199–2210.

Bejnordi, B. E., Veta, M., Van Diest, P. J., Van Ginneken, B., Karssemeijer, N., Litjens, G., Van Der Laak, J. A., Hermsen, M., Manson, Q. F., Balkenhol, M. et al. (2017b). Diagnostic assessment of deep learning algorithms for detection of lymph node metastases in women with breast cancer, *JAMA* **318**(22): 2199–2210.

Belharbi, S., Rony, J., Dolz, J., Ayed, I. B., McCaffrey, L. and Granger, E. (2021). Deep interpretable classification and weakly-supervised segmentation of histology images via max-min uncertainty, *IEEE Transactions on Medical Imaging*.

Belkin, M., Niyogi, P. and Sindhwani, V. (2005). On manifold regularization, *International Workshop on Artificial Intelligence and Statistics*, PMLR, pp. 17–24.

Belkin, M., Niyogi, P. and Sindhwani, V. (2006). Manifold regularization: A geometric framework for learning from labeled and unlabeled examples., *Journal of Machine Learning Research* **7**(11).

Blum, A. and Mitchell, T. (1998). Combining labeled and unlabeled data with co-training, *Proceedings of the Eleventh Annual Conference on Computational Learning Theory*, pp. 92–100.

Boyd, J., Liashuha, M., Deutsch, E., Paragios, N., Christodoulidis, S. and Vakalopoulou, M. (2021). Self-supervised representation learning using visual field expansion on digital pathology, *Proceedings of the IEEE/CVF International Conference on Computer Vision*, pp. 639–647.

Bulten, W., Pinckaers, H., van Boven, H., Vink, R., de Bel, T., van Ginneken, B., van der Laak, J., Hulsbergen-van de Kaa, C. and Litjens, G. (2020). Automated deep-learning system for gleason grading of prostate cancer using biopsies: a diagnostic study, *The Lancet Oncology* **21**(2): 233–241.

Campanella, G., Hanna, M. G., Geneslaw, L., Miraflor, A., Werneck Krauss Silva, V., Busam, K. J., Brogi, E., Reuter, V. E., Klimstra, D. S. and Fuchs, T. J. (2019). Clinical-grade computational pathology using weakly supervised deep learning on whole slide images, *Nature Medicine* **25**(8): 1301–1309.

Caron, M., Misra, I., Mairal, J., Goyal, P., Bojanowski, P. and Joulin, A. (2020). Unsupervised learning of visual features by contrasting cluster assignments, *Advances in Neural Information Processing Systems* **33**: 9912–9924.

Caron, M., Touvron, H., Misra, I., Jégou, H., Mairal, J., Bojanowski, P. and Joulin, A. (2021). Emerging properties in self-supervised vision transformers, *Proceedings of the IEEE/CVF International Conference on Computer Vision*, pp. 9650–9660.

Chang, C.-C. and Lin, C.-J. (2011). Libsvm: a library for support vector machines, *ACM Transactions on Intelligent Systems and Technology (TIST)* **2**(3): 1–27.

Chaudhary, K., Poirion, O. B., Lu, L. and Garmire, L. X. (2018). Deep learning-based multi-omics integration robustly predicts survival in liver cancer, *Clinical Cancer Research* **24**(6): 1248–1259.

Chen, H., Qi, X., Yu, L., Dou, Q., Qin, J. and Heng, P.-A. (2017). Dcan: Deep contour-aware networks for object instance segmentation from histology images, *Medical Image Analysis* **36**: 135–146.

Chen, L., Bentley, P., Mori, K., Misawa, K., Fujiwara, M. and Rueckert, D. (2019). Self-supervised learning for medical image analysis using image context restoration, *Medical Image Analysis* **58**: 101539.

Chen, R. J. and Krishnan, R. G. (2022). Self-supervised vision transformers learn visual concepts in histopathology, *arXiv preprint arXiv:2203.00585* .

Chen, R. J., Lu, N. I. and Mahmood, F. (2020). Pathomic fusion: an integrated framework for fusing histopathology and genomic features for cancer diagnosis and prognosis, *IEEE Transactions on Medical Imaging* .

Chen, T., Kornblith, S., Norouzi, M. and Hinton, G. (2020). A simple framework for contrastive learning of visual representations, *International Conference on Machine Learning*, PMLR, pp. 1597–1607.

Chen, X., Fan, H., Girshick, R. and He, K. (2020). Improved baselines with momentum contrastive learning, *arXiv preprint arXiv:2003.04297* .

Chen, X. and He, K. (2021). Exploring simple siamese representation learning, *Proceedings of the IEEE/CVF Conference on Computer Vision and Pattern Recognition*, pp. 15750–15758.

Chen, Z., Wang, T., Wu, X., Hua, X.-S., Zhang, H. and Sun, Q. (2022). Class re-activation maps for weakly-supervised semantic segmentation, *arXiv preprint arXiv:2203.00962* .

Chen, Z., Zhang, J., Che, S., Huang, J., Han, X. and Yuan, Y. (2021). Diagnose like a pathologist: Weakly-supervised pathologist-tree network for slide-level immunohistochemical scoring, *35th AAAI Conference on Artificial Intelligence (AAAI-21)*, AAAI Press, pp. 47–54.

Cheng, H.-T., Yeh, C.-F., Kuo, P.-C., Wei, A., Liu, K.-C., Ko, M.-C., Chao, K.-H., Peng, Y.-C. and Liu, T.-L. (2020). Self-similarity student for partial label histopathology image segmentation, *European Conference on Computer Vision*, Springer, pp. 117–132.

Chhipa, P. C., Upadhyay, R., Pihlgren, G. G., Saini, R., Uchida, S. and Liwicki, M. (2022). Magnification prior: A self-supervised method for learning representations on breast cancer histopathological images, *arXiv preprint arXiv:2203.07707* .

Chikontwe, P., Kim, M., Nam, S. J., Go, H. and Park, S. H. (2020). Multiple instance learning with center embeddings for histopathology classification, *International Conference on Medical Image Computing and Computer-Assisted Intervention*, Springer, pp. 519–528.

Chong, Y., Ding, Y., Yan, Q. and Pan, S. (2020). Graph-based semi-supervised learning: A review, *Neurocomputing* **408**: 216–230.

Cifci, D., Foersch, S. and Kather, J. N. (2022). Artificial intelligence to identify genetic alterations in conventional histopathology, *The Journal of Pathology* .

Ciga, O., Xu, T. and Martel, A. L. (2022). Self supervised contrastive learning for digital histopathology, *Machine Learning with Applications* **7**: 100198.

Clark, K., Vendt, B., Smith, K., Freymann, J., Kirby, J., Koppel, P., Moore, S., Phillips, S., Maffitt, D., Pringle, M. et al. (2013). The cancer imaging archive (tcia): maintaining and operating a public information repository, *Journal of Digital Imaging* **26**(6): 1045–1057.

Cong, C., Liu, S., Ieva, A. D., Pagnucco, M., Berkovsky, S. and Song, Y. (2021). Semi-supervised adversarial learning for stain normalisation in histopathology images, *International Conference on Medical Image Computing and Computer-Assisted Intervention*, Springer, pp. 581–591.

Coudray, N., Ocampo, P. S., Sakellaropoulos, T., Narula, N., Snuderl, M., Fenyö, D., Moreira, A. L., Razavian, N. and Tsirigos, A. (2018). Classification and mutation prediction from non-small cell lung cancer histopathology images using deep learning, *Nature Medicine* **24**(10): 1559–1567.

Cruz-Roa, A., Basavanhally, A., González, F., Gilmore, H., Feldman, M., Ganesan, S., Shih, N., Tomaszewski, J. and Madabhushi, A. (2014). Automatic detection of invasive ductal carcinoma in whole slide images with convolutional neural networks, *Medical Imaging 2014: Digital Pathology*, Vol. 9041, SPIE, p. 904103.

Cruz-Roa, A., Gilmore, H., Basavanhally, A., Feldman, M., Ganesan, S., Shih, N. N., Tomaszewski, J., González, F. A. and Madabhushi, A. (2017). Accurate and reproducible invasive breast cancer detection in whole-slide images: a deep learning approach for quantifying tumor extent, *Scientific Reports* **7**(1): 1–14.

Dai, Z., Yang, Z., Yang, F., Cohen, W. W. and Salakhutdinov, R. R. (2017). Good semi-supervised learning that requires a bad gan, *Advances in Neural Information Processing Systems* **30**.

Dara, R., Kremer, S. C. and Stacey, D. A. (2002). Clustering unlabeled data with soms improves classification of labeled real-world data, *Proceedings of the 2002 International Joint Conference on Neural Networks. IJCNN'02 (Cat. No. 02CH37290)*, Vol. 3, IEEE, pp. 2237–2242.

Decencière, E., Zhang, X., Cazuguel, G., Lay, B., Cochener, B., Trone, C., Gain, P., Ordonez, R., Massin, P., Erginay, A. et al. (2014). Feedback on a publicly distributed image database: the messidor database, *Image Analysis & Stereology* **33**(3): 231–234.

Dehaene, O., Camara, A., Moindrot, O., de Lavergne, A. and Courtiol, P. (2020). Self-supervision closes the gap between weak and strong supervision in histology, *arXiv preprint arXiv:2012.03583* .

Demiriz, A., Bennett, K. P. and Embrechts, M. J. (1999). Semi-supervised clustering using genetic algorithms, *Artificial Neural Networks in Engineering (ANNIE-99)* pp. 809–814.

Deng, J., Dong, W., Socher, R., Li, L.-J., Li, K. and Fei-Fei, L. (2009). Imagenet: A large-scale hierarchical image database, *2009 IEEE Conference on Computer Vision and Pattern Recognition*, Ieee, pp. 248–255.

Ding, K., Liu, Q., Lee, E., Zhou, M., Lu, A. and Zhang, S. (2020). Feature-enhanced graph networks for genetic mutational prediction using histopathological images in colon cancer, *International Conference on Medical Image Computing and Computer-Assisted Intervention*, Springer, pp. 294–304.

Doersch, C., Gupta, A. and Efros, A. A. (2015). Unsupervised visual representation learning by context prediction, *Proceedings of the IEEE International Conference on Computer Vision*, pp. 1422–1430.

Donahue, J., Krähenbühl, P. and Darrell, T. (2016). Adversarial feature learning, *arXiv preprint arXiv:1605.09782* .

Dong, X., Bao, J., Zhang, T., Chen, D., Zhang, W., Yuan, L., Chen, D., Wen, F. and Yu, N. (2021). Poco: Perceptual codebook for bert pre-training of vision transformers, *arXiv preprint arXiv:2111.12710* .

Doyle, S., Hwang, M., Shah, K., Madabhushi, A., Feldman, M. and Tomaszewski, J. (2007). Automated grading of prostate cancer using architectural and textural image features, *2007 4th IEEE International Symposium on Biomedical Imaging: From Nano to Macro*, IEEE, pp. 1284–1287.

Doyle, S., Rodriguez, C., Madabhushi, A., Tomaszewski, J. and Feldman, M. (2006). Detecting prostatic adenocarcinoma from digitized histology using a multi-scale hierarchical classification approach, *2006 International Conference of the IEEE Engineering in Medicine and Biology Society*, IEEE, pp. 4759–4762.

Ehteshami Bejnordi, B., Mullooly, M., Pfeiffer, R. M., Fan, S., Vacek, P. M., Weaver, D. L., Herschorn, S., Brinton, L. A., van Ginneken, B., Karssemeijer, N. et al. (2018). Using deep convolutional neural networks to identify and classify tumor-associated stroma in diagnostic breast biopsies, *Modern Pathology* **31**(10): 1502–1512.

Erhan, D., Courville, A., Bengio, Y. and Vincent, P. (2010). Why does unsupervised pre-training help deep learning?, *Proceedings of the Thirteenth International Conference on Artificial Intelligence and Statistics*, JMLR Workshop and Conference Proceedings, pp. 201–208.

Feng, J. and Zhou, Z.-H. (2017). Deep mml network, *Proceedings of the AAAI Conference on Artificial Intelligence*, Vol. 31.

Foucart, A., Debeir, O. and Decaestecker, C. (2019). Snow: Semi-supervised, noisy and/or weak data for deep learning in digital pathology, *2019 IEEE 16th International Symposium on Biomedical Imaging (ISBI 2019)*, IEEE, pp. 1869–1872.

Fu, Y., Jung, A. W., Torne, R. V., Gonzalez, S., Vöhringer, H., Shmatko, A., Yates, L. R., Jimenez-Linan, M., Moore, L. and Gerstung, M. (2020). Pan-cancer computational histopathology reveals mutations, tumor composition and prognosis, *Nature Cancer* **1**(8): 800–810.

Gelasca, E. D., Byun, J., Obara, B. and Manjunath, B. (2008). Evaluation and benchmark for biological image segmentation, *2008 15th IEEE International Conference on Image Processing*, IEEE, pp. 1816–1819.

Gertych, A., Ing, N., Ma, Z., Fuchs, T. J., Salman, S., Mohanty, S., Bhele, S., Velásquez-Vacca, A., Amin, M. B. and Knudsen, B. S. (2015). Machine learning approaches to analyze histological images of tissues from radical prostatectomies, *Computerized Medical Imaging and Graphics* **46**: 197–208.

Gidaris, S., Singh, P. and Komodakis, N. (2018). Unsupervised representation learning by predicting image rotations, *arXiv preprint arXiv:1803.07728* .

Goldberg, A., Zhu, X., Singh, A., Xu, Z. and Nowak, R. (2009). Multi-manifold semi-supervised learning, *Artificial Intelligence and Statistics*, PMLR, pp. 169–176.

Goodfellow, I. (2016). Nips 2016 tutorial: Generative adversarial networks, *arXiv preprint arXiv:1701.00160* .

Goodfellow, I., Bengio, Y., Courville, A. and Bengio, Y. (2016). Deep learning, volume 1.

Goodfellow, I., Pouget-Abadie, J., Mirza, M., Xu, B., Warde-Farley, D., Ozair, S., Courville, A. and Bengio, Y. (2014). Generative adversarial nets, *Advances in Neural Information Processing Systems* **27**.

Grill, J.-B., Strub, F., Altché, F., Tallec, C., Richemond, P., Buchatskaya, E., Doersch, C., Avila Pires, B., Guo, Z., Gheshlaghi Azar, M. et al. (2020). Bootstrap your own latent-a new approach to self-supervised learning, *Advances in Neural Information Processing Systems* **33**: 21271–21284.

Gu, F., Burlutskiy, N., Andersson, M. and Wilén, L. K. (2018). Multi-resolution networks for semantic segmentation in whole slide images, *Computational Pathology and Ophthalmic Medical Image Analysis*, Springer, pp. 11–18.

Guinney, J., Dienstmann, R., Wang, X., De Reynies, A., Schlicker, A., Soneson, C., Marisa, L., Roepman, P., Nyamundanda, G., Angelino, P. et al. (2015). The consensus molecular subtypes of colorectal cancer, *Nature Medicine* **21**(11): 1350–1356.

Gurcan, M. N., Boucheron, L. E., Can, A., Madabhushi, A., Rajpoot, N. M. and Yener, B. (2009). Histopathological image analysis: A review, *IEEE Reviews in Biomedical Engineering* **2**: 147–171.

Haeusser, P., Mordvintsev, A. and Cremers, D. (2017). Learning by association—a versatile semi-supervised training method for neural networks, *Proceedings of the IEEE Conference on Computer Vision and Pattern Recognition*, pp. 89–98.

Halicek, M., Shahedi, M., Little, J. V., Chen, A. Y., Myers, L. L., Sumer, B. D. and Fei, B. (2019). Head and neck cancer detection in digitized whole-slide histology using convolutional neural networks, *Scientific Reports* **9**(1): 1–11.

Hashimoto, N., Fukushima, D., Koga, R., Takagi, Y., Ko, K., Kohno, K., Nakaguro, M., Nakamura, S., Hontani, H. and Takeuchi, I. (2020). Multi-scale domain-adversarial multiple-instance cnn for cancer subtype classification with unannotated histopathological images, *Proceedings of the IEEE/CVF Conference on Computer Vision and Pattern Recognition*, pp. 3852–3861.

He, K., Chen, X., Xie, S., Li, Y., Dollár, P. and Girshick, R. (2021). Masked autoencoders are scalable vision learners, *arXiv preprint arXiv:2111.06377* .

He, K., Fan, H., Wu, Y., Xie, S. and Girshick, R. (2020). Momentum contrast for unsupervised visual representation learning, *Proceedings of the IEEE/CVF Conference on Computer Vision and Pattern Recognition*, pp. 9729–9738.

Hou, L., Nguyen, V., Kanevsky, A. B., Samaras, D., Kurc, T. M., Zhao, T., Gupta, R. R., Gao, Y., Chen, W., Foran, D. et al. (2019). Sparse autoencoder for unsupervised nucleus detection and representation in histopathology images, *Pattern Recognition* **86**: 188–200.

Hou, L., Samaras, D., Kurc, T. M., Gao, Y., Davis, J. E. and Saltz, J. H. (2016). Patch-based convolutional neural network for whole slide tissue image classification, *Proceedings of the IEEE Conference on Computer Vision and Pattern Recognition*, pp. 2424–2433.

Ilse, M., Tomczak, J. and Welling, M. (2018). Attention-based deep multiple instance learning, *International Conference on Machine Learning*, PMLR, pp. 2127–2136.

Jafari-Khouzani, K. and Soltanian-Zadeh, H. (2003). Multiwavelet grading of pathological images of prostate, *IEEE Transactions on Biomedical Engineering* **50**(6): 697–704.

Jaiswal, A. K., Panshin, I., Shulkin, D., Aneja, N. and Abramov, S. (2019). Semi-supervised learning for cancer detection of lymph node metastases, *arXiv preprint arXiv:1906.09587*.

Kandemir, M., Zhang, C. and Hamprecht, F. A. (2014). Empowering multiple instance histopathology cancer diagnosis by cell graphs, *International Conference on Medical Image Computing and Computer-Assisted Intervention*, Springer, pp. 228–235.

Kandoth, C., McLellan, M. D., Vandin, F., Ye, K., Niu, B., Lu, C., Xie, M., Zhang, Q., McMichael, J. F., Wyczalkowski, M. A. et al. (2013). Mutational landscape and significance across 12 major cancer types, *Nature* **502**(7471): 333–339.

Kapil, A., Meier, A., Zuraw, A., Steele, K. E., Rebelatto, M. C., Schmidt, G. and Brieu, N. (2018). Deep semi supervised generative learning for automated tumor proportion scoring on nsclc tissue needle biopsies, *Scientific Reports* **8**(1): 1–10.

Kather, J. N., Heij, L. R., Grabsch, H. I., Loeffler, C., Echle, A., Muti, H. S., Krause, J., Niehues, J. M., Sommer, K. A., Bankhead, P. et al. (2020). Pan-cancer image-based detection of clinically actionable genetic alterations, *Nature Cancer* **1**(8): 789–799.

Kather, J. N., Krisam, J., Charoentong, P., Luedde, T., Herpel, E., Weis, C.-A., Gaiser, T., Marx, A., Valous, N. A., Ferber, D. et al. (2019). Predicting survival from colorectal cancer histology slides using deep learning: A retrospective multicenter study, *PLoS Medicine* **16**(1): e1002730.

Kather, J. N., Pearson, A. T., Halama, N., Jäger, D., Krause, J., Loosen, S. H., Marx, A., Boor, P., Tacke, F., Neumann, U. P. et al. (2019). Deep learning can predict microsatellite instability directly from histology in gastrointestinal cancer, *Nature Medicine* **25**(7): 1054–1056.

Kather, J. N., Weis, C.-A., Bianconi, F., Melchers, S. M., Schad, L. R., Gaiser, T., Marx, A. and Zöllner, F. G. (2016). Multi-class texture analysis in colorectal cancer histology, *Scientific Reports* **6**(1): 1–11.

Kingma, D. P. and Welling, M. (2013). Auto-encoding variational bayes, *arXiv preprint arXiv:1312.6114*.

Kleppe, A., Skrede, O.-J., De Raedt, S., Liestøl, K., Kerr, D. J. and Danielsen, H. E. (2021). Designing deep learning studies in cancer diagnostics, *Nature Reviews Cancer* **21**(3): 199–211.

Koohbanani, N. A., Unnikrishnan, B., Khurram, S. A., Krishnaswamy, P. and Rajpoot, N. (2021). Self-path: Self-supervision for classification of pathology images with limited annotations, *IEEE Transactions on Medical Imaging* **40**(10): 2845–2856.

Kraus, O. Z., Ba, J. L. and Frey, B. J. (2016). Classifying and segmenting microscopy images with deep multiple instance learning, *Bioinformatics* **32**(12): i52–i59.

Kumar, N., Verma, R., Sharma, S., Bhargava, S., Vahadane, A. and Sethi, A. (2017). A dataset and a technique for generalized nuclear segmentation for computational pathology, *IEEE Transactions on Medical Imaging* **36**(7): 1550–1560.

Laine, S. and Aila, T. (2016). Temporal ensembling for semi-supervised learning, *arXiv preprint arXiv:1610.02242*.

Larsen, A. B. L., Sønderby, S. K., Larochelle, H. and Winther, O. (2016). Autoencoding beyond pixels using a learned similarity metric, *International Conference on Machine Learning*, PMLR, pp. 1558–1566.

Lee, D.-H. et al. (2013). Pseudo-label: The simple and efficient semi-supervised learning method for deep neural networks, *Workshop on Challenges in Representation Learning, ICML*, Vol. 3, p. 896.

Lee, J., Kim, E. and Yoon, S. (2021). Anti-adversarially manipulated attributions for weakly and semi-supervised semantic segmentation, *Proceedings of the IEEE/CVF Conference on Computer Vision and Pattern Recognition*, pp. 4071–4080.

Lerousseau, M., Vakalopoulou, M., Classe, M., Adam, J., Battistella, E., Carré, A., Estienne, T., Henry, T., Deutsch, E. and Paragios, N. (2020). Weakly supervised multiple instance learning histopathological tumor segmentation, *International Conference on Medical Image Computing and Computer-Assisted Intervention*, Springer, pp. 470–479.

Li, B., Li, Y. and Eliceiri, K. W. (2021). Dual-stream multiple instance learning network for whole slide image classification with self-supervised contrastive learning, *Proceedings of the IEEE/CVF Conference on Computer Vision and Pattern Recognition*, pp. 14318–14328.

Li, F., Yang, Y., Wei, Y., He, P., Chen, J., Zheng, Z. and Bu, H. (2021). Deep learning-based predictive biomarker of pathological complete response to neoadjuvant chemotherapy from histological images in breast cancer, *Journal of Translational Medicine* **19**(1): 1–13.

Li, H., Yang, F., Zhao and Yao, J. (2021). Dt-mil: Deformable transformer for multi-instance learning on histopathological image, *International Conference on Medical Image Computing and Computer-Assisted Intervention*, Springer, pp. 206–216.

Li, J., Speier, W., Ho, K. C., Sarma, K. V., Gertych, A., Knudsen, B. S. and Arnold, C. W. (2018). An em-based semi-supervised deep learning approach for semantic segmentation of histopathological images from radical prostatectomies, *Computerized Medical Imaging and Graphics* **69**: 125–133.

Liu, S., Shah, Z., Sav, A., Russo, C., Berkovsky, S., Qian, Y., Coiera, E. and Di Ieva, A. (2020). Isocitrate dehydrogenase (idh) status prediction in histopathology images of gliomas using deep learning, *Scientific Reports* **10**(1): 1–11.

Liu, X., Zhang, F., Hou, Z., Mian, L., Wang, Z., Zhang, J. and Tang, J. (2021). Self-supervised learning: Generative or contrastive, *IEEE Transactions on Knowledge and Data Engineering* .

Ljosa, V., Sokolnicki, K. L. and Carpenter, A. E. (2012). Annotated high-throughput microscopy image sets for validation, *Nature methods* **9**(7): 637–637.

Lu, M. Y., Chen, R. J., Wang, J., Dillon, D. and Mahmood, F. (2019). Semi-supervised histology classification using deep multiple instance learning and contrastive predictive coding, *arXiv preprint arXiv:1910.10825* .

Lu, M. Y., Williamson, D. F., Chen, T. Y., Chen, R. J., Barbieri, M. and Mahmood, F. (2021). Data-efficient and weakly supervised computational pathology on whole-slide images, *Nature Biomedical Engineering* **5**(6): 555–570.

Luo, X., Zang, X., Yang, L., Huang, J., Liang, F., Rodriguez-Canales, J., Wistuba, I. I., Gazdar, A., Xie, Y. and Xiao, G. (2017). Comprehensive computational pathological image analysis predicts lung cancer prognosis, *Journal of Thoracic Oncology* **12**(3): 501–509.

Madabhushi, A. and Lee, G. (2016). Image analysis and machine learning in digital pathology: Challenges and opportunities, *Medical Image Analysis* **33**: 170–175.

Mahapatra, D., Bozorgtabar, B., Thiran, J.-P. and Shao, L. (2020). Structure preserving stain normalization of histopathology images using self supervised semantic guidance, *International Conference on Medical Image Computing and Computer-Assisted Intervention*, Springer, pp. 309–319.

Marini, N., Otálora, S., Müller, H. and Atzori, M. (2021). Semi-supervised training of deep convolutional neural networks with heterogeneous data and few local annotations: An experiment on prostate histopathology image classification, *Medical Image Analysis* **73**: 102165.

Maron, O. and Lozano-Pérez, T. (1997). A framework for multiple-instance learning, *Advances in Neural Information Processing Systems* **10**.

Martel, A., Nofech-Mozes, S., Salama, S., Akbar, S. and Peikari, M. (2019). Assessment of residual breast cancer cellularity after neoadjuvant chemotherapy using digital pathology [data set], *The Cancer Imaging Archive* .

Melekhov, I., Kannala, J. and Rahtu, E. (2016). Siamese network features for image matching, *2016 23rd International Conference on Pattern Recognition (ICPR)*, IEEE, pp. 378–383.

Mercan, C., Aksoy, S., Mercan, E., Shapiro, L. G., Weaver, D. L. and Elmore, J. G. (2017). Multi-instance multi-label learning for multi-class classification of whole slide breast histopathology images, *IEEE Transactions on Medical Imaging* **37**(1): 316–325.

Muhammad, H., Sigel, C. S., Campanella, G., Boerner, T., Pak, L. M., Büttner, S., IJzermans, J. N., Koerkamp, B. G., Doukas, M., Jarnagin, W. R. et al. (2019). Unsupervised subtyping of cholangiocarcinoma using a deep clustering convolutional autoencoder, *International Conference on Medical Image Computing and Computer-Assisted Intervention*, Springer, pp. 604–612.

Murthy, V., Hou, L., Samaras, D., Kurc, T. M. and Saltz, J. H. (2017). Center-focusing multi-task cnn with injected features for classification of glioma nuclear images, *2017 IEEE Winter Conference on Applications of Computer Vision (WACV)*, IEEE, pp. 834–841.

Myronenko, A., Xu, Z., Yang, D., Roth, H. R. and Xu, D. (2021). Accounting for dependencies in deep learning based multiple instance learning for whole slide imaging, *International Conference on Medical Image Computing and Computer-Assisted Intervention*, Springer, pp. 329–338.

Nagpal, K., Foote, D., Liu, Y., Chen, P.-H. C., Wulczyn, E., Tan, F., Olson, N., Smith, J. L., Mohtashamian, A., Wren, J. H. et al. (2019). Development and validation of a deep learning algorithm for improving gleason scoring of prostate cancer, *NPJ Digital Medicine* **2**(1): 1–10.

Naik, N., Madani, A., Esteva, A., Keskar, N. S., Press, M. F., Ruderman, D., Agus, D. B. and Socher, R. (2020). Deep learning-enabled breast cancer hormonal receptor status determination from base-level h&e stains, *Nature Communications* **11**(1): 1–8.

Naylor, P., Laé, M., Reyal, F. and Walter, T. (2018). Segmentation of nuclei in histopathology images by deep regression of the distance map, *IEEE Transactions on Medical Imaging* **38**(2): 448–459.

Noroozi, M. and Favaro, P. (2016). Unsupervised learning of visual representations by solving jigsaw puzzles, *European Conference on Computer Vision*, Springer, pp. 69–84.

Odena, A. (2016). Semi-supervised learning with generative adversarial networks, *arXiv preprint arXiv:1606.01583* .

Pan, J., Bi, Q., Yang, Y., Zhu, P. and Bian, C. (2022). Label-efficient hybrid-supervised learning for medical image segmentation, *arXiv preprint arXiv:2203.05956* .

Parag, T., Plaza, S. and Scheffer, L. (2014). Small sample learning of superpixel classifiers for em segmentation, *International Conference on Medical Image Computing and Computer-Assisted Intervention*, Springer, pp. 389–397.

Pathak, D., Krahenbuhl, P., Donahue, J., Darrell, T. and Efros, A. A. (2016). Context encoders: Feature learning by inpainting, *Proceedings of the IEEE Conference on Computer Vision and Pattern Recognition*, pp. 2536–2544.

Peikari, M., Salama, S., Nofech-Mozes, S. and Martel, A. L. (2018). A cluster-then-label semi-supervised learning approach for pathology image classification, *Scientific Reports* **8**(1): 1–13.

Petrick, N. A., Akbar, S., Cha, K. H., Nofech-Mozes, S., Sahiner, B., Gavrielides, M. A., Kalpathy-Cramer, J., Drukier, K., Martel, A. L. et al. (2021). Spie-aapm-nci breastpathq challenge: an image analysis challenge for quantitative tumor cellularity assessment in breast cancer histology images following neoadjuvant treatment, *Journal of Medical Imaging* **8**(3): 034501.

Qaiser, T., Sirinukunwattana, K., Nakane, K., Tsang, Y.-W., Epstein, D. and Rajpoot, N. (2016). Persistent homology for fast tumor segmentation in whole slide histology images, *Procedia Computer Science* **90**: 119–124.

Qu, H., Wu, P., Huang, Q., Yi, J., Yan, Z., Li, K., Riedlinger, G. M., De, S., Zhang, S. and Metaxas, D. N. (2020). Weakly supervised deep nuclei segmentation using partial points annotation in histopathology images, *IEEE Transactions on Medical Imaging* **39**(11): 3655–3666.

Qu, L., Luo, X., Liu, S., Wang, M. and Song, Z. (2022). Dgmil: Distribution guided multiple instance learning for whole slide image classification, *arXiv preprint arXiv:2206.08861*.

Quiros, A. C., Coudray, N., Yeaton, A., Sunhem, W., Murray-Smith, R., Tsirigos, A. and Yuan, K. (2021). Adversarial learning of cancer tissue representations, *arXiv preprint arXiv:2108.02223*.

Quiros, A. C., Murray-Smith, R. and Yuan, K. (2019). Pathologygan: Learning deep representations of cancer tissue, *arXiv preprint arXiv:1907.02644*.

Qureshi, H., Sertel, O., Rajpoot, N., Wilson, R. and Gurcan, M. (2008). Adaptive discriminant wavelet packet transform and local binary patterns for meningioma subtype classification, *International Conference on Medical Image Computing and Computer-Assisted Intervention*, Springer, pp. 196–204.

Radford, A., Metz, L. and Chintala, S. (2015). Unsupervised representation learning with deep convolutional generative adversarial networks, *arXiv preprint arXiv:1511.06434*.

Rajpoot, K. and Rajpoot, N. (2004). Svm optimization for hyperspectral colon tissue cell classification, *International Conference on Medical Image Computing and Computer-Assisted Intervention*, Springer, pp. 829–837.

Ramon, J. and De Raedt, L. (2000). Multi instance neural networks, *Proceedings of the ICML-2000 Workshop on Attribute-value and Relational Learning*, pp. 53–60.

Rethlefsen, M. L., Kirtley, S., Waffenschmidt, S., Ayala, A. P., Moher, D., Page, M. J. and Koffel, J. B. (2021). Prismas: an extension to the prisma statement for reporting literature searches in systematic reviews, *Systematic Reviews* **10**(1): 1–19.

Rifai, S., Dauphin, Y. N., Vincent, P., Bengio, Y. and Muller, X. (2011). The manifold tangent classifier, *Advances in Neural Information Processing Systems* **24**.

Rifai, S., Vincent, P., Muller, X., Glorot, X. and Bengio, Y. (2011). Contractive auto-encoders: Explicit invariance during feature extraction, *International Conference on Machine Learning*.

Rony, J., Belharbi, S., Dolz, J., Ayed, I. B., McCaffrey, L. and Granger, E. (2019). Deep weakly-supervised learning methods for classification and localization in histology images: a survey, *arXiv preprint arXiv:1909.03354*.

Ru, L., Zhan, Y., Yu, B. and Du, B. (2022). Learning affinity from attention: End-to-end weakly-supervised semantic segmentation with transformers, *arXiv preprint arXiv:2203.02664*.

Sahasrabudhe, M., Christodoulidis, S., Salgado, R., Michiels, S., Loi, S., André, F., Paragios, N. and Vakalopoulou, M. (2020). Self-supervised nuclei segmentation in histopathological images using attention, *International Conference on Medical Image Computing and Computer-Assisted Intervention*, Springer, pp. 393–402.

Saillard, C., Dehaene, O., Marchand, T., Moindrot, O., Kamoun, A., Schmauch, B. and Jegou, S. (2021). Self supervised learning improves dmmr/msi detection from histology slides across multiple cancers, *arXiv preprint arXiv:2109.05819*.

Saillard, C., Schmauch, B., Laifa, O., Moarii, M., Toldo, S., Zaslavskiy, M., Pronier, E., Laurent, A., Amaddeo, G., Regnault, H. et al. (2020). Predicting survival after hepatocellular carcinoma resection using deep learning on histological slides, *Hepatology* **72**(6): 2000–2013.

Salimans, T., Goodfellow, I., Zaremba, W., Cheung, V., Radford, A. and Chen, X. (2016). Improved techniques for training gans, *Advances in Neural Information Processing Systems* **29**.

Shaban, M., Khurram, S. A., Fraz, M. M., Alsubaie, N., Masood, I., Mushtaq, S., Hassan, M., Loya, A. and Rajpoot, N. M. (2019). A novel digital score for abundance of tumour infiltrating lymphocytes predicts disease free survival in oral squamous cell carcinoma, *Scientific Reports* **9**(1): 1–13.

Shao, Z., Bian, H., Chen, Y., Wang, Y., Zhang, J., Ji, X. et al. (2021). Transmil: Transformer based correlated multiple instance learning for whole slide image classification, *Advances in Neural Information Processing Systems* **34**.

Sharma, Y., Shrivastava, A., Ehsan, L., Moskaluk, C. A., Syed, S. and Brown, D. (2021). Cluster-to-conquer: A framework for end-to-end multi-instance learning for whole slide image classification, *Medical Imaging with Deep Learning*, PMLR, pp. 682–698.

Shaw, S., Pajak, M., Lisowska, A., Tsaftaris, S. A. and O’Neil, A. Q. (2020). Teacher-student chain for efficient semi-supervised histology image classification, *arXiv preprint arXiv:2003.08797*.

Shi, X., Sapkota, M., Xing, F., Liu, F., Cui, L. and Yang, L. (2018). Pairwise based deep ranking hashing for histopathology image classification and retrieval, *Pattern Recognition* **81**: 14–22.

Shi, X., Su, H., Xing, G. and Yang, L. (2020). Graph temporal ensembling based semi-supervised convolutional neural network with noisy labels for histopathology image analysis, *Medical Image Analysis* **60**: 101624.

Shi, X., Xing, F., Xie, Y., Zhang, Z., Cui, L. and Yang, L. (2020). Loss-based attention for deep multiple instance learning, *Proceedings of the AAAI Conference on Artificial Intelligence*, Vol. 34, pp. 5742–5749.

Shurab, S. and Duwairi, R. (2021). Self-supervised learning methods and applications in medical imaging analysis: A survey, *arXiv preprint arXiv:2109.08685*.

Singh, S., Janoos, F., Péicot, T., Caserta, E., Leone, G., Rittscher, J. and Machiraju, R. (2011). Identifying nuclear phenotypes using semi-supervised metric learning, *Biennial International Conference on Information Processing in Medical Imaging*, Springer, pp. 398–410.

Sirinukunwattana, K., Pluim, J. P., Chen, H., Qi, X., Heng, P.-A., Guo, Y. B., Wang, L. Y., Matuszewski, B. J., Bruni, E., Sanchez, U. et al. (2017). Gland segmentation in colon histology images: The glas challenge contest, *Medical Image Analysis* **35**: 489–502.

Sirinukunwattana, K., Raza, S. E. A., Tsang, Y.-W., Snead, D. R., Cree, I. A. and Rajpoot, N. M. (2016). Locality sensitive deep learning for detection and classification of nuclei in routine colon cancer histology images, *IEEE transactions on medical imaging* **35**(5): 1196–1206.

Skrede, O.-J., De Raedt, S., Kleppe, A., Hveem, T. S., Liestøl, K., Maddison, J., Askautrud, H. A., Pradhan, M., Nesheim, J. A., Albregtsen, F. et al. (2020). Deep learning for prediction of colorectal cancer outcome: a discovery and validation study, *The Lancet* **395**(10221): 350–360.

Spanhol, F. A., Oliveira, L. S., Petitjean, C. and Heutte, L. (2015). A dataset for breast cancer histopathological image classification, *IEEE Transactions on Biomedical Engineering* **63**(7): 1455–1462.

Sparks, R. and Madabhushi, A. (2016). Out-of-sample extrapolation utilizing semi-supervised manifold learning (ose-ssl): content based image retrieval for histopathology images, *Scientific Reports* **6**(1): 1–15.

Srinidhi, C. L., Ciga, O. and Martel, A. L. (2021). Deep neural network models for computational histopathology: A survey, *Medical Image Analysis* **67**: 101813.

Srinidhi, C. L., Kim, S. W., Chen, F.-D. and Martel, A. L. (2022). Self-supervised driven consistency training for annotation efficient histopathology image analysis, *Medical Image Analysis* **75**: 102256.

Stacke, K., Unger, J., Lundström, C. and Eilertsen, G. (2021). Learning representations with contrastive self-supervised learning for histopathology applications, *arXiv preprint arXiv:2112.05760*.

Su, H., Shi, X., Cai, J. and Yang, L. (2019). Local and global consistency regularized mean teacher for semi-supervised nuclei classification, *International Conference on Medical Image Computing and Computer-Assisted Intervention*, Springer, pp. 559–567.

Su, H., Yin, Z., Huh, S., Kanade, T. and Zhu, J. (2015). Interactive cell segmentation based on active and semi-supervised learning, *IEEE Transactions on Medical Imaging* **35**(3): 762–777.

Su, L., Liu, Y., Wang, M. and Li, A. (2021). Semi-hic: A novel semi-supervised deep learning method for histopathological image classification, *Computers in Biology and Medicine* **137**: 104788.

Swiderska-Chadaj, Z., Pinckaers, H., van Rijthoven, M., Balkenhol, M., Melnikova, M., Geessink, O., Manson, Q., Sherman, M., Polonia, A., Parry, J. et al. (2019). Learning to detect lymphocytes in immunohistochemistry with deep learning, *Medical Image Analysis* **58**: 101547.

Tajbakhsh, N., Jeyaseelan, L., Li, Q., Chiang, J. N., Wu, Z. and Ding, X. (2020). Embracing imperfect datasets: A review of deep learning solutions for medical image segmentation, *Medical Image Analysis* **63**: 101693.

Tarvainen, A. and Valpola, H. (2017). Mean teachers are better role models: Weight-averaged consistency targets improve semi-supervised deep learning results, *Advances in Neural Information Processing Systems* **30**.

TCGA (2019). The cancer genome atlas, <https://www.cancer.gov/tcga>.

Team, N. L. S. T. R. et al. (2011). The national lung screening trial: overview and study design, *Radiology* **258**(1): 243.

Tellez, D., Litjens, G., van der Laak, J. and Ciompi, F. (2019). Neural image compression for gigapixel histopathology image analysis, *IEEE Transactions on Pattern Analysis and Machine Intelligence* **43**(2): 567–578.

Tolkach, Y., Dohmögörén, T., Toma, M. and Kristiansen, G. (2020). High-accuracy prostate cancer pathology using deep learning, *Nature Machine Intelligence* **2**(7): 411–418.

Tomita, N., Abdollahi, B., Wei, J., Ren, B., Suriawinata, A. and Hassanpour, S. (2019). Attention-based deep neural networks for detection of cancerous and precancerous esophagus tissue on histopathological slides, *JAMA Network Open* **2**(11): e1914645–e1914645.

Tu, M., Huang, J., He, X. and Zhou, B. (2019). Multiple instance learning with graph neural networks, *arXiv preprint arXiv:1906.04881*.

Van den Oord, A., Li, Y. and Vinyals, O. (2018). Representation learning with contrastive predictive coding, *arXiv e-prints* pp. arXiv–1807.

Van Engelen, J. E. and Hoos, H. H. (2020). A survey on semi-supervised learning, *Machine Learning* **109**(2): 373–440.

Veeling, B. S., Linmans, J., Winkens, J., Cohen, T. and Welling, M. (2018). Rotation equivariant cnns for digital pathology, *International Conference on Medical Image Computing and Computer-assisted Intervention*, Springer, pp. 210–218.

Velmahos, C. S., Badgeley, M. and Lo, Y.-C. (2021). Using deep learning to identify bladder cancers with fgfr-activating mutations from histology images, *Cancer Medicine* **10**(14): 4805–4813.

Veta, M., Heng, Y. J., Stathonikos, N., Bejnordi, B. E., Beca, F., Wollmann, T., Rohr, K., Shah, M. A., Wang, D., Rousson, M. et al. (2019). Predicting breast tumor proliferation from whole-slide images: the tupac16 challenge, *Medical Image Analysis* **54**: 111–121.

Vincent, P., Larochelle, H., Bengio, Y. and Manzagol, P.-A. (2008). Extracting and composing robust features with denoising autoencoders, *Proceedings of the 25th International Conference on Machine Learning*, pp. 1096–1103.

Wang, C.-W., Lee, Y.-C., Calista, E., Zhou, F., Zhu, H., Suzuki, R., Komura, D., Ishikawa, S. and Cheng, S.-P. (2018). A benchmark for comparing precision medicine methods in thyroid cancer diagnosis using tissue microarrays, *Bioinformatics* **34**(10): 1767–1773.

Wang, X., Chen, H., Gan, C., Lin, H., Dou, Q., Tsougenis, E., Huang, Q., Cai, M. and Heng, P.-A. (2019). Weakly supervised deep learning for whole slide lung cancer image analysis, *IEEE Transactions on Cybernetics* **50**(9): 3950–3962.

Wang, X., Yan, Y., Tang, P., Bai, X. and Liu, W. (2018). Revisiting multiple instance neural networks, *Pattern Recognition* **74**: 15–24.

Wang, X., Yang, S., Zhang, J., Wang, M., Zhang, J., Huang, J., Yang, W. and Han, X. (2021). Transpath: Transformer-based self-supervised learning for histopathological image classification, *International Conference on Medical Image Computing and Computer-Assisted Intervention*, Springer, pp. 186–195.

Ward, R. L. and Hawkins, N. J. (2015). Molecular and cellular oncology (mco) study tumour collection, *UNSW Australia*.

Wei, J. W., Tafe, L. J., Linnik, Y. A., Vaickus, L. J., Tomita, N. and Hassanpour, S. (2019). Pathologist-level classification of histologic patterns on resected lung adenocarcinoma slides with deep neural networks, *Scientific Reports* **9**(1): 1–8.

Wessels, F., Schmitt, M., Krieghoff-Henning, E., Jutzi, T., Worst, T. S., Waldbillig, F., Neuberger, M., Maron, R. C., Steeg, M., Gaiser, T. et al. (2021). Deep learning approach to predict lymph node metastasis directly from primary tumour histology in prostate cancer, *BJU International* **128**(3): 352–360.

Weston, J., Ratle, F., Mobahi, H. and Collobert, R. (2012). Deep learning via semi-supervised embedding, *Neural Networks: Tricks of the Trade*, Springer, pp. 639–655.

Woerl, A.-C., Eckstein, M., Geiger, J., Wagner, D. C., Daher, T., Stenzel, P., Fernandez, A., Hartmann, A., Wand, M., Roth, W. et al. (2020). Deep learning predicts molecular subtype of muscle-invasive bladder cancer from conventional histopathological slides, *European Urology* **78**(2): 256–264.

Wu, J., Yu, Y., Huang, C. and Yu, K. (2015). Deep multiple instance learning for image classification and auto-annotation, *Proceedings of the IEEE Conference on Computer Vision and Pattern Recognition*, pp. 3460–3469.

Xie, Q., Dai, Z., Hovy, E., Luong, T. and Le, Q. (2020). Unsupervised data augmentation for consistency training, *Advances in Neural Information Processing Systems* **33**: 6256–6268.

Xie, X., Chen, J., Li, K. and Zheng, Y. (2020). Instance-aware self-supervised learning for nuclei segmentation, *International Conference on Medical Image Computing and Computer-assisted Intervention*, Springer, pp. 341–350.

Xu, G., Song, Z., Sun, Z., Ku, C., Yang, Z., Liu, C., Wang, S., Ma, J. and Xu, W. (2019). Camel: A weakly supervised learning framework for histopathology image segmentation, *Proceedings of the IEEE/CVF International Conference on Computer Vision*, pp. 10682–10691.

Xu, J., Hou, J., Zhang, Y., Feng, R., Ruan, C., Zhang, T. and Fan, W. (2020). Data-efficient histopathology image analysis with deformation representation learning, *2020 IEEE International Conference on Bioinformatics and Biomedicine (BIBM)*, IEEE, pp. 857–864.

Xu, K., Su, H., Zhu, J., Guan, J.-S. and Zhang, B. (2016). Neuron segmentation based on cnn with semi-supervised regularization, *Proceedings of the IEEE Conference on Computer Vision and Pattern Recognition Workshops*, pp. 20–28.

Xu, L., Ouyang, W., Bennamoun, M., Boussaid, F. and Xu, D. (2022). Multi-class token transformer for weakly supervised semantic segmentation, *arXiv preprint arXiv:2203.02891*.

Yalniz, I. Z., Jégou, H., Chen, K., Paluri, M. and Mahajan, D. (2019). Billion-scale semi-supervised learning for image classification, *arXiv preprint arXiv:1905.00546*.

Yan, Y., Wang, X., Guo, X., Fang, J., Liu, W. and Huang, J. (2018). Deep multi-instance learning with dynamic pooling, *Asian Conference on Machine Learning*, PMLR, pp. 662–677.

Yang, J., Ju, J., Guo, L., Ji, B., Shi, S., Yang, Z., Gao, S., Yuan, X., Tian, G., Liang, Y. et al. (2022). Prediction of her2-positive breast cancer recurrence and metastasis risk from histopathological images and clinical information via multimodal deep learning, *Computational and Structural Biotechnology Journal* **20**: 333–342.

Yang, L., Zhang, Y., Chen, J., Zhang, S. and Chen, D. Z. (2017). Suggestive annotation: A deep active learning framework for biomedical image segmentation, *International Conference on Medical Image Computing and Computer-assisted Intervention*, Springer, pp. 399–407.

Yang, P., Hong, Z., Yin, X., Zhu, C. and Jiang, R. (2021). Self-supervised visual representation learning for histopathological images, *International Conference on Medical Image Computing and Computer-Assisted Intervention*, Springer, pp. 47–57.

Yang, P., Zhai, Y., Li, L., Lv, H., Wang, J., Zhu, C. and Jiang, R. (2020). A deep metric learning approach for histopathological image retrieval, *Methods* **179**: 14–25.

Yao, J., Zhu, X., Jonnagaddala, J., Hawkins, N. and Huang, J. (2020). Whole slide images based cancer survival prediction using attention guided deep multiple instance learning networks, *Medical Image Analysis* **65**: 101789.

Yu, K.-H., Zhang, C., Berry, G. J., Altman, R. B., Ré, C., Rubin, D. L. and Snyder, M. (2016). Predicting non-small cell lung cancer prognosis by fully automated microscopic pathology image features, *Nature Communications* **7**(1): 1–10.

Zhang, R., Isola, P. and Efros, A. A. (2016). Colorful image colorization, *European Conference on Computer Vision*, Springer, pp. 649–666.

Zhang, Y., Yang, L., Chen, J., Fredericksen, M., Hughes, D. P. and Chen, D. Z. (2017). Deep adversarial networks for biomedical image segmentation utilizing unannotated images, *International Conference on Medical Image Computing and Computer-assisted Intervention*, Springer, pp. 408–416.

Zhao, Y., Yang, F., Fang, Y., Liu, H., Zhou, N., Zhang, J., Sun, J., Yang, S., Menze, B., Fan, X. et al. (2020). Predicting lymph node metastasis using histopathological images based on multiple instance learning with deep graph convolution, *Proceedings of the IEEE/CVF Conference on Computer Vision and Pattern Recognition*, pp. 4837–4846.

Zheng, H., Yang, L., Chen, J., Han, J., Zhang, Y., Liang, P., Zhao, Z., Wang, C. and Chen, D. Z. (2019). Biomedical image segmentation via representative annotation, *Proceedings of the AAAI Conference on Artificial Intelligence*, Vol. 33, pp. 5901–5908.

Zhou, Y., Chen, H., Lin, H. and Heng, P.-A. (2020). Deep semi-supervised knowledge distillation for overlapping cervical cell instance segmentation, *International Conference on Medical Image Computing and Computer-Assisted Intervention*, Springer, pp. 521–531.

Zhou, Z.-H. and Li, M. (2005). Tri-training: Exploiting unlabeled data using three classifiers, *IEEE Transactions on Knowledge and Data Engineering* **17**(11): 1529–1541.

Zhou, Z., Sodha, V., Pang, J., Gotway, M. B. and Liang, J. (2021). Models genesis, *Medical Image Analysis* **67**: 101840.

Zhu, X. J. (2005). Semi-supervised learning literature survey, *CS Technical Reports* .

Zhu, X., Yao, J., Zhu, F. and Huang, J. (2017). Wsisa: Making survival prediction from whole slide histopathological images, *Proceedings of the IEEE Conference on Computer Vision and Pattern Recognition*, pp. 7234–7242.